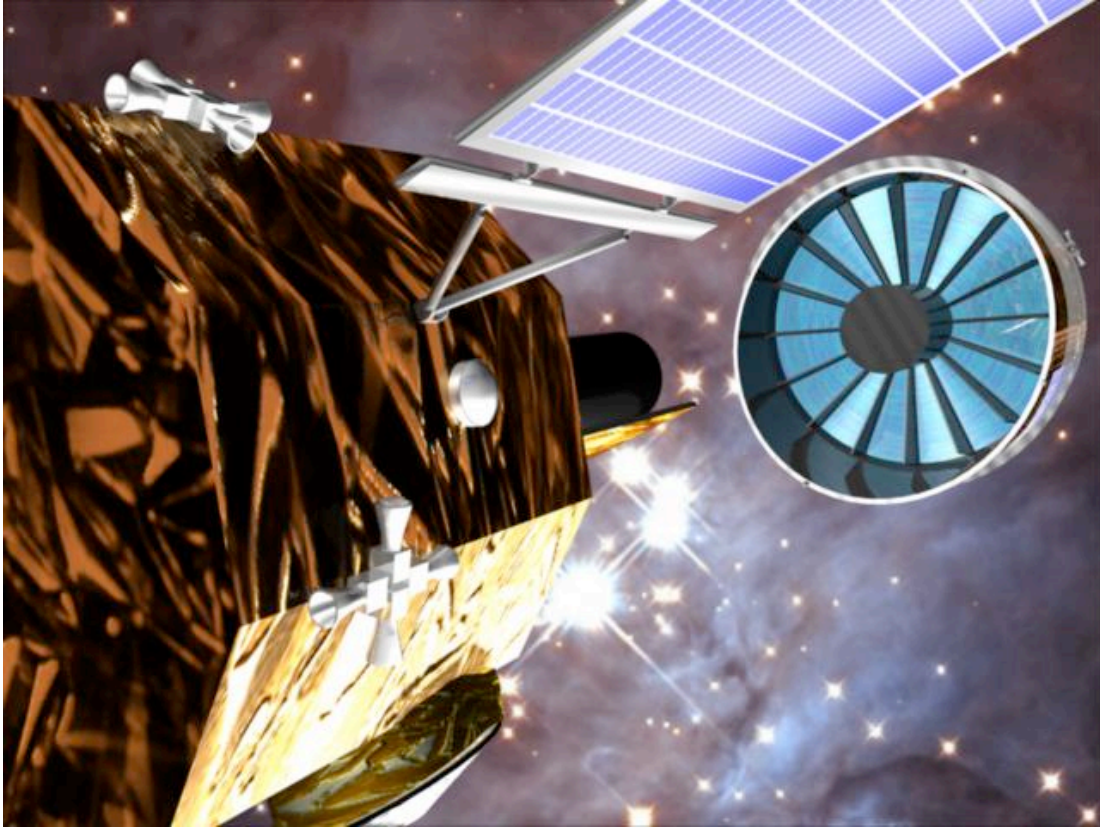


XEUS

Physics of the Hot Evolving Universe



Principal Investigators

Martin Turner, Department of Physics and Astronomy, University of Leicester, UK

Günther Hasinger, Max-Planck-Institut für extraterrestrische Physik, Garching, Germany

Co-Investigators

Monique Arnaud, CEA/DSM/DAPNIA/SAP CEN-Saclay, France ; **Xavier Barcons**, (CSIC-UC), Santander, Spain; **Didier Barret**, CESR, CNRS/UPS, Toulouse, France; **Mark Bautz**, MIT, Cambridge, USA; **Johan Bleeker**, SRON/U. Utrecht, Netherlands; **Hans Böhringer**, MPE Garching, Germany; **Thomas Boller**, MPE Garching, Germany; **William Nielsen Brandt**, Penn. State U. University Park, USA; **Francisco Carrera**, (CSIC-UC), Santander, Spain; **Massimo Cappi**, INAF-IASF, Bologna, Italy; **Andrea Comastri**, INAF, Oss. Astron. Bologna, Italy; **Enrico Costa**, U. La Sapienza, Rome, Italy; **Thierry Courvoisier**, ISDC, Geneva, Switzerland; **Piet de Korte**, SRON, Utrecht, Netherlands; **Andrew Fabian**, Institute of Astronomy, Cambridge, UK; **Kathryn Flanagan**, MIT, Cambridge, USA; **Richard Griffiths**, Carnegie Mellon U., Pittsburgh, USA; **Jelle Kaastra**, SRON, Utrecht, Netherlands; **Steve Kahn**, KIPAC, SLAC, Stanford U., USA; **Richard Kelley**, NASA GSFC, Greenbelt, USA; **Hideyo Kunieda**, ISAS/JAXA, Sagamihara, Japan; **Kazuo Makishima**, U. Tokyo, Japan; **Giorgio Matt**, U. Roma Tre, Rome, Italy; **Mariano Mendez**, SRON, Utrecht, Netherlands; **Kazuhisa Mitsuda**, ISAS/JAXA, Sagamihara, Japan; **Kirpal Nandra**, Imperial College, London, UK; **Takaya Ohashi**, Tokyo Metropolitan U., Japan; **Giorgio Palumbo**, INAF, Oss. Astron. Bologna, Italy; **Mikhail Pavlinsky**, IKI, Moscow, Russia; **Salvatore Sciortino**, INAF, Oss. Astr. Palermo, Italy; **Alan Smith**, MSSL, UCL, UK; **Lothar Strüder**, MPE Garching, MPI-HLL, Germany; **Tadayuki Takahashi**, ISAS/JAXA, Sagamihara, Japan; **Yoshi Ueda**, ISAS/JAXA, Sagamihara, Japan; **Jacco Vink**, U. Utrecht, Netherlands; **Robert Warwick**, U. Leicester, UK; **Mike Watson**, U. Leicester, UK; **Richard Willingale**, U. Leicester, UK; **Nan Shuang Zhang**, Tsinghua U., IHEP, Beijing, China.

Table of Contents

1	Executive summary	1
2	Introduction	2
3	Scientific objectives	4
3.1	Co-evolution of galaxies and their supermassive black holes	4
3.2	Evolution of large scale structure and nucleosynthesis	7
3.3	Matter under extreme conditions	9
3.4	Dynamics and chemistry of cosmic plasmas	12
3.5	Requirements on the proposed payload	14
4	Mission profile	14
4.1	Launcher requirements	14
4.2	Orbit requirements	15
4.3	Ground segment requirements	15
4.4	Special requirements.....	15
5	Instrument payload	15
5.1	Model payload.....	15
5.2	Sensitivity Calculation	17
5.3	Key characteristics of instruments.....	17
5.4	Pointing and alignment requirements for focal plane instruments.....	24
5.5	Operational modes	25
5.6	Calibration requirements	25
5.7	Special requirements.....	25
5.8	Current heritage and technology readiness	25
6	Spacecraft key factors	26
6.1	Spacecraft configuration.....	26
6.2	AOCS requirements	28
6.3	On-board data handling and telemetry requirements.....	28
6.4	Mission operations concept (ground segment).....	29
6.5	Estimated overall resources (mass and power).....	29
6.6	Specific environmental constraints (EMC, temperature, cleanliness)	29
6.7	Current heritage and technology readiness level	29
6.8	Proposed procurement approach & international partners	29
6.9	Critical issues	29
7	Science operations and archiving	30
8	Key technology areas	30
8.1	Current development status.....	30
8.2	Essential future developments.....	31
9	Communications and outreach	32
10	References	32
11	XEUS supporters	33
12	Letters of support	34

1 Executive summary

The X-ray Evolving Universe Spectroscopy mission, XEUS, is Europe's next generation X-ray observatory, designed to address two of the four main questions posed in Cosmic Vision, namely: *What are the fundamental laws of the Universe?* and, *How did the Universe originate, and what is it made of?* XEUS will be the observatory best suited to tackle at least three of the twelve major topics laid down in Cosmic Vision: *The evolving violent Universe. The Universe taking shape. and Matter under extreme conditions.* With unprecedented sensitivity to the hot, million-degree Universe, XEUS will provide the long-sought answers to key questions in contemporary astrophysics:

- How did supermassive black holes form and grow?
- How did feedback from these black holes influence galaxy growth?
- How did large scale structure evolve?
- How did the baryonic component of this structure become chemically enriched?
- How does gravity behave in the strong field limit?

XEUS will constitute a cornerstone element in the *dual track* approach towards the study of formation of structure, which requires us to study simultaneously the evolution of the hot and cold components of the Universe. In this sense, XEUS is fully complementary to the major future ground- and space-based observatories, JWST, LISA, ALMA, ELT and SKA. X-rays can penetrate through obscuring gas and dust in the centres of young galaxies and so can disentangle the ambiguity between star-formation and accretion power in the evolving Universe. Dark matter, which can currently only be studied through its gravitational action on visible matter, can be probed through the evolution of large scale structures, traced by the hot X-ray-emitting gas trapped in the dark matter potential wells. While significant progress has been made in constraining the cosmological parameters and in reconstructing the large-scale structure of the dark matter distribution, we still lack even a basic understanding of the spatial and chemical evolution of the baryonic component of the Universe. XEUS is needed both to observe directly the evolution of the warm/hot baryonic matter in the intergalactic medium and the hot plasma in galaxy clusters, and to trace galaxy evolution through the effects of energy release and nucleosynthesis in the intergalactic medium. The most extreme physical conditions in the Universe, i.e. regions with the strongest gravity, the highest densities, the hottest temperatures and the largest magnetic fields, occur in the immediate vicinity of black holes and in neutron stars. Since X-rays constitute the major component of radiation from the innermost parts of the accretion flow and from compact surfaces, XEUS will give answers to open questions like: how does gravity work in the strong field limit, what are the properties of curved spacetime, and what is the equation of state of (supra)nuclear matter?

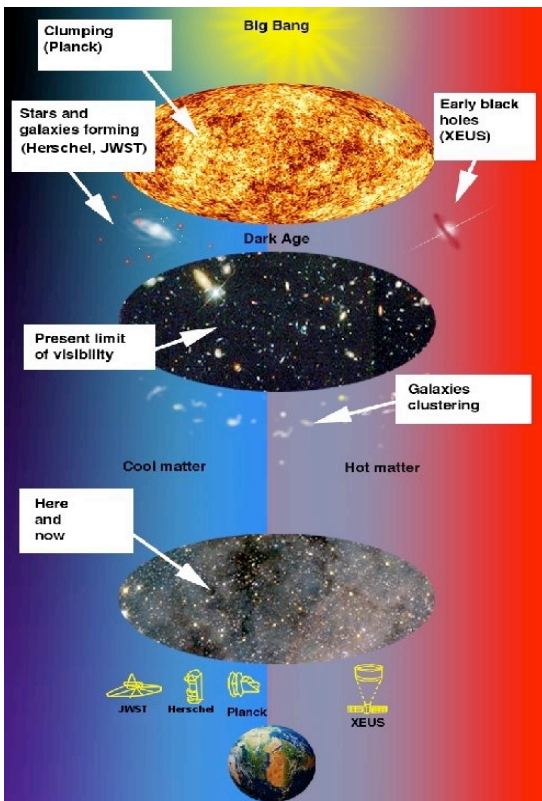
XEUS will be placed in a halo orbit at L2, by a single Ariane 5 ECA, and comprises two spacecraft. The optics assembly of XEUS is contained in the Mirror Spacecraft (MSC) while a suite of five focal plane instruments is contained in the Detector Spacecraft (DSC), which is maintained at the focus of the mirror by *formation flying*. L2 provides the necessary benign gravity gradient environment for formation flying and also allows efficient thermal control of the optics and instruments, and long continuous observations. The main requirement for XEUS is to provide a focused beam of X-rays with an effective aperture of 5 m² at 1 keV and a spatial resolution better than 5 arcsec half-energy width. This is achieved using silicon micro-pore optics, which give an advantage, in terms of mass/unit collecting area, of more than an order of magnitude compared to the largest current X-ray telescope, aboard XMM-Newton. There are two major focal plane instruments. The cryogenic imaging spectrometer (NFI) uses an array of superconducting Transition Edge Sensors to give energy resolution of 2 to 6 eV FWHM, over the energy range 0.1–8 keV, combined with imaging over a field of view (FoV) of 1.6 arcmin square. The Wide Field Imager (WFI), based on silicon pixel arrays, has a FoV of 7 arcmin (goal 10 arcmin) square, with 30 to 150 eV energy resolution. These two instruments are supplemented with three smaller instruments, which are needed to address specific science aims of XEUS. The Hard X-ray Imager (HXI) extends the energy range up to 40 keV to establish continuum spectra at the peak of the X-ray background accurately, and to explore acceleration phenomena in cosmic plasmas; the High Time Resolution Spectrometer (HTRS) enables XEUS to monitor sub-millisecond variations in the emission from local black holes and neutron stars, in order to study matter under extreme conditions; and the X-ray POLarimeter (XPOL) will for the first time allow the diagnostic power of X-ray polarisation to be exploited. The required instrument cooling will not use expendable cryogens, and the power system will be designed for ten years of life, as will expendables for manoeuvring and formation flying.

The XEUS MSC requires only standard 3-axis stabilization with modest accuracy. The DSC however requires a *formation flying package* which will maintain the boresight between the instruments and the mirror within the required tolerances, i.e. better than 2.5 mm along the optical axis and better than 0.5 arcsec absolute attitude

measurement accuracy. Given the two spacecraft configuration for XEUS, X-rays originating from the sky area outside of the telescope FoV could contribute to the instrument background. A long baffle (7.9 m) of 1.0 m diameter, integrated as a structural member of the DSC, in combination with a skirt mounted on the MSC is therefore required. The total wet mass of the MSC and the DSC, supplemented by the launcher adapter, amounts to 6.5 tons, compliant with the Ariane 5 ECA launch capability (6.6 tons). An observatory of this capability, launched more than a decade hence, should make use of the most advanced technology in order to be future-proof and to realise its great potential. The basic requirements for the XEUS instrumentation and optical technology have already been demonstrated at proof-of-principle level and we are confident that reasonable additional developments can ensure the science goals. For example, a proof of concept has been demonstrated for the micro-pore optics, indicating that the required performance can be met. The XEUS *mirror assembly*, the *cryogenics cooling chain* and the *DSC formation flying package* remain the major development tasks. A fully accessible public archive of data will be created and maintained in order to maximise the scientific output of the mission.

As noted in the proposal call, XEUS falls outside the cost envelope of L-class missions and requires international participation. In terms of major contributions to the mission, Japan has been a collaborator from the beginning of the project with an interest in participating at the system level, e.g. via provision of the DSC or the cryogenics chain, and also at the payload level, like a contribution to the X-ray optics and the focal plane sensor assembly. Russia has also indicated that they want to investigate a major contribution to XEUS such as the provision of the MSC and participation in payload elements. Formal letters expressing these intentions were sent to ESA. Because of the on-going NASA Beyond Einstein Programme Assessment Committee review, an inter-agency agreement with the US cannot be considered within 2007; but scientists from the US are co-investigators, and we expect to elaborate a more formal agreement during the study phase, if XEUS is selected. China also has a keen interest in the XEUS science, manifested by a supporting letter from its Academy. Two explicit scenarios are given, detailing the CaC as distributed over ESA, international partners and national funding agencies. The first scenario entails the provision of the DSC by Japan, the second scenario the provision of the MSC by Russia and the cryogenic chain by Japan. The payload would be procured by international teams, led by PIs, using national funds.

2 Introduction



Astrophysics and Cosmology are currently in a “Golden Age”. Precision measurements have determined the cosmic geometry and history. After an early inflationary phase dark energy, dark matter and hot baryons emerge as the three dominating forms of matter and energy density in the contemporary Universe. The study of the inflationary phase will gain another important boost with a successful launch of the Planck mission in 2008. An in-depth and coherent investigation of the formation and evolution of structure in the Universe will require a highly sensitive “*dual track*” observational approach studying both the cold baryonic matter and, in a fully complementary manner, the evolution of hot baryonic matter (see adjacent cartoon). The formation of structure from cold matter on the stellar/galaxy mass scale can be probed primarily at infrared and (sub)millimeter wavelengths by e.g. the Herschel, JWST and ALMA observatories. X-ray observations are uniquely suited to studying the warm/hot baryons embedded in the dark matter potential wells of the cosmic web.

It has become increasingly apparent that the formation of supermassive black holes in Active Galactic Nuclei (AGN) is an integral feature of the galaxy formation process. Theory, observations and numerical N-body simulations all suggest that AGN outflows may be the crucial link responsible for

regulation of star formation in massive galaxies, but the details of these processes are as yet completely unclear, due to lack of quantitative information. The first black holes must have originated at high redshifts $z=10-15$. By far the best way to discover high redshift black holes is through X-ray observations, due to the strong contrast with

the host galaxy and relative immunity to obscuration. Black holes with masses in the range 10^6 – 10^9 solar masses will have X-ray luminosities of $10^{42.5}$ – $10^{44.5}$ ergs s^{-1} and studying their growth and evolution with redshift can only be achieved with highly-sensitive imaging X-ray spectroscopy.

Imaging X-ray spectroscopy is also the essential tool to address structure formation on mass scales much larger than individual galaxies. This is amply evidenced by the scale of hot intracluster gas seen in the rich clusters of galaxies encountered in the local Universe, where the hot gas represents about five times the baryonic content contained in the total of all the constituent galaxies in the cluster. Models for structure formation in the Universe, starting from the seed inhomogeneities, indicate that the major fraction of matter in the contemporary Universe is hot with temperatures in the range 10^5 – 10^6 K. A significant amount of additional energy may also have been fed back into the intergalactic medium, heating the Universe even more. This dominant hot matter component, which evolves simultaneously with the cool matter observed at infrared and sub-millimeter wavelengths, can only be traced through high-resolution X-ray spectroscopy.

The physics of matter under extreme conditions, like accreting hot plasma close to the event horizon of black holes or outflowing relativistic jets in active galactic nuclei, will also be probed, as will be the equation of state of baryonic matter in neutron stars, with possible links to the strong interaction and the Standard Model.

The key scientific goals for this next generation X-ray observatory, in the context of the Cosmic Vision programme, can be summarized as follows:

- Detect the earliest (super)massive black holes and study their growth and evolution. Significant constraints on the origin and growth of massive black holes can only be derived if deep X-ray observations probe the redshift range $z = 5$ – 10 . This imposes an unprecedented demand on acquiring a limiting sensitivity in keV-X-rays around 3×10^{-18} ergs $cm^{-2}s^{-1}$. [*The evolving violent Universe*]
- Study the first gravitationally bound dark-matter dominated systems and trace their evolution to the present epoch, since they potentially constitute the dominant fraction of the current mass density of baryons in the Universe. This requires the spectral sensitivity to detect prominent X-ray spectral features in moderately enriched (small) clusters out to $z \sim 2$. Determine the mass, density, temperature and metallicity of the true intergalactic medium. This requires unprecedented *spectral grasp*: a *critical* combination of high X-ray collecting power and X-ray spectral resolving power. [*The Universe taking shape*]
- Observe matter under extreme physical conditions to address topics of great interest in contemporary physics: gravity in the strong field limit, supranuclear densities, extreme magnetic field strengths and relativistic acceleration. This requires the use of sensitive, time-resolved X-ray emission line spectroscopy, fast timing and polarimetry. This requires unprecedented instantaneous photon collecting power, i.e. operation in the photon-limited regime for fast time resolved spectroscopic measurements. [*Matter under extreme conditions*]

These ambitious science goals can be met with the following key observatory characteristics:

- A spectroscopic collecting area of > 5 m^2 at 1 keV and > 2 m^2 at 7 keV
- An angular resolution better than 5 arcsec, targeted at 2 arcsec to avoid source confusion in reaching a limiting point source sensitivity of 3×10^{-18} ergs $cm^{-2}s^{-1}$ in the 0.5–2 keV band.
- A spectral resolution ranging from 2–6 eV in the 0.1–8 keV energy band.
- An energy bandpass of 0.1–40 keV and ultra-fast timing and polarimetric capabilities.

To accommodate these characteristics, a suite of focal plane instruments in conjunction with a high-throughput grazing incidence X-ray mirror system is proposed (section 5). The required X-ray grazing incidence optics needs a minimum focal length of ~ 35 m to provide > 5 m^2 effective area at 1 keV and arcsec angular resolution. For such a focal length, a *dual* spacecraft configuration is essential: it comprises a Mirror Spacecraft (MSC) and a Detector Spacecraft (DSC). The focal plane sensors comprise a Wide Field Imaging camera (WFI) for detection of the soft and medium energy X-rays, a wide field Hard X-ray Imager (HXI) and a Narrow Field Imaging X-ray spectrometer (NFI). Dedicated instruments for ultra-fast timing (HTRS) and sensitive X-ray polarimetry (XPOL) complement the focal plane assembly. The DSC maintains the prime focal plane instrument at the focus of the mirror using *formation flying*. The science requirements imposed on the instrument complement are summarized in table 3.1. The proposed concept provides a large, long-lived X-ray telescope facility, which, building on recently achieved technological break-throughs, meets the scientific challenges in an optimum, timely, and highly cost-effective way.

3 Scientific objectives

3.1 Co-evolution of galaxies and their supermassive black holes

A key goal of XEUS is to study the evolving violent Universe by tracing mass accretion onto black holes throughout cosmic time out to the highest possible redshifts. In this context XEUS will tackle the following challenges:

- Discover the first $10^6 M_{\text{sun}}$ black holes at $z \geq 10$, thought to be QSO seeds in starbursting protogalaxies.
- Detect and characterize Compton-thick Seyfert galaxies at redshifts of $z=2-3$.
- Study the role that AGN feedback plays in the co-evolution and downsizing of black holes and galaxies.
- Study the cosmic evolution of iron lines and black hole spins.

The first black holes

Following recombination at $z \sim 1000$ primordial structures formed where gravity overpowered the pressure of the ambient baryons, eventually creating the first stars. Ultimately the first stellar mass black holes ($\sim 100 M_{\text{sun}}$) must have formed in explosions of the most massive stars, likely associated with gamma-ray bursts. Whereas the WMAP results show that the Universe was substantially re-ionized by stars and protogalaxies at $z \sim 10-14$, the highest redshift galaxies, quasars and gamma-ray bursts which are currently known are all in the range $z=6-7$. The search for even higher redshift objects therefore holds the key to our understanding of this crucial phase in the development of the Universe. Growing supermassive black holes even at $z=6-7$ (i.e. in < 1 Gyr) represents a challenge for theoretical models, because it requires an Eddington- or even super-Eddington limited exponential accretion over many folding times. However, recent gas-dynamical cosmological simulations are able to produce the first quasars with $10^{9.5} M_{\text{sun}}$ at $z=6.5$ through a rapid sequence of mergers in small groups of protogalaxies [1].

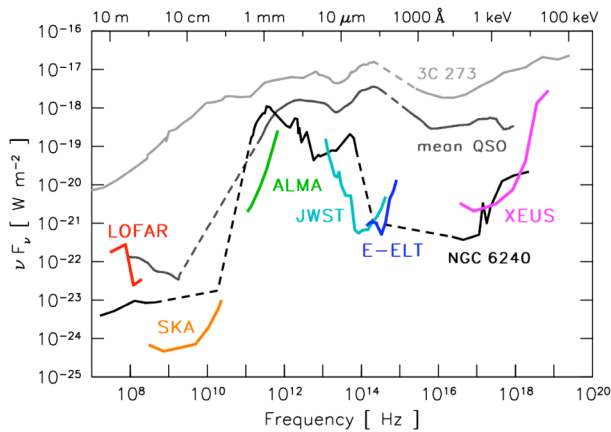


Fig. 3.1: XEUS sensitivity compared to other major future facilities. Spectral energy distributions for 3C273, for an average QSO template, and for the obscured starforming merger NGC 6240 are shown at a redshift of $z=10$. Sensitivities assume $1 \text{ Ms } 5\sigma$ detections for XEUS and equivalent $12 \text{ h } 1\sigma$ detections for the other instruments.

The growth is likely to proceed in a self-regulated manner owing to feedback with the progenitor host galaxies which are expected to experience a period of intense star formation and obscured accretion, preceding the optically bright quasar phase. The complex physics involved in such a scenario is poorly understood and indeed the same simulations suggest that supermassive ($> 10^9 M_{\text{sun}}$) objects might be extremely rare. On the other hand, Chandra and XMM-Newton found no evolution in the quasar accretion mode, which stays approximately constant at a few tenths of the Eddington limit out to $z \geq 6$. In order to accommodate the very short timescale available to build up supermassive black holes in the early Universe, a drastic change in the accretion properties may have occurred above $z \sim 6-7$. However it is very likely that BH as massive as $10^6 M_{\text{sun}}$ hosted by vigorously star forming

galaxies, existed as early as $z=10-11$. XEUS is uniquely configured to discover and study these objects, which are rendered invisible in other wavebands due to intergalactic absorption and dilution by their host galaxy. To detect X-ray emitting black holes out to $z \geq 10$ and to investigate their growth requires an unprecedented combination of large throughput, high angular resolution and large FoV in the X-ray regime. To generate an X-ray luminosity $> 10^{42.5} \text{ erg s}^{-1}$, which is needed to discriminate an accreting black hole from the vigorously star forming host galaxy, requires a black hole mass of $> 10^6 M_{\text{sun}}$ (assuming a typical spectral energy distribution). At $z=10$ this corresponds to an X-ray flux $> 3 \times 10^{-18} \text{ erg cm}^{-2} \text{ s}^{-1}$. This is the main science driver for the large effective area and sets the angular resolution for the XEUS mission to better than 5 arcsec. At this flux limit about 100(10) AGN per deg^2 are expected at $z > 6(10)$ [2]. This sensitivity is also well matched to that of future optical/infrared (E-ELT and JWST) and radio/sub-mm (SKA and ALMA) telescopes. Fig. 3.1 compares the sensitivity of future ground and space based telescopes from the radio to X-rays with the spectral energy distribution of several AGN scaled to a redshift $z=10$. Even though ALMA and/or JWST will be able to detect $z \sim 10$ objects, only sensitive X-ray observations will be able to properly disentangle the power associated with black hole accretion from that due to star formation. A prototypical example is NGC 6240, where a powerful starburst and two heavily obscured Compton-thick accreting Black Holes coexist.

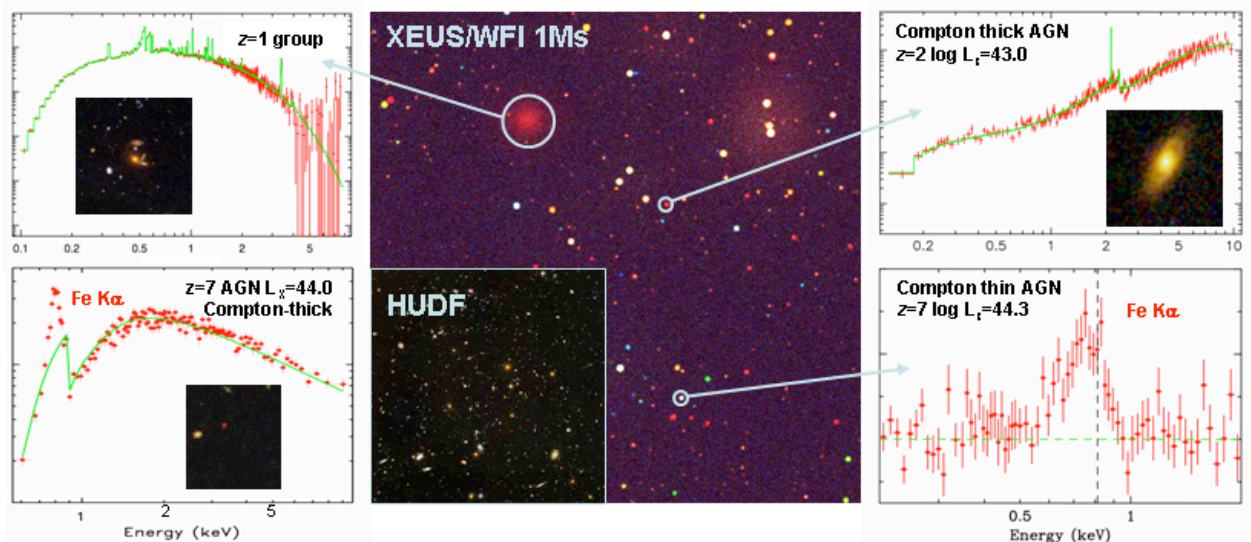


Figure 3.2: Simulation of a 1 Ms XEUS WFI observation of the Chandra Deep Field South (CDFS). We assume a PSF HEW of $2''$. Real CDFS sources have been augmented with fainter, absorbed AGN based on the latest X-ray background synthesis model [2], and a population of starburst galaxies based on the GOODS/Spitzer $24\ \mu\text{m}$ data. The HST ACS Ultradeep Field, the deepest optical image so far, is shown as an insert. To the left and right are X-ray spectra for different objects from the same simulation. The upper left shows the spectrum ($\sqrt{F_{\text{V}}}$ space, arbitrary units) of a known high redshift ($z\sim 1$) galaxy group. The upper right shows a $z=2$ Compton-thick object with $L_X = 10^{43}\ \text{erg s}^{-1}$. The HST image (inset) shows a bulge galaxy - these kinds of AGN may be optically invisible but can dominate the obscured accretion budget of the universe. Slightly more luminous examples can be detected by XEUS, and their redshifts determined solely from the X-ray spectra, out to $z=7$ (bottom left). At the bottom right we show a data/model ratio for a type-1 (unobscured) AGN at the same redshift with $L_X = 2 \times 10^{44}\ \text{erg s}^{-1}$. We simulate a narrow Fe-K α emission line with a rest frame equivalent width of 200 eV plus an accretion disk line with parameters similar to MCG-6-30-15 ($EW=300\ \text{eV}$). Though challenging even for XEUS, there is the prospect that we might measure relativistic effects in the iron lines of individual AGN out to the dark ages of the universe.

Obscured black hole growth

Ultimately, we wish to characterise the evolution of black hole accretion over the whole of cosmic time, by combining ultra-deep with wider field X-ray observations to uncover accreting black holes over a broad range of redshifts and luminosities. In the theoretical framework above, most of the accretion at high redshift is expected to be heavily obscured. Observational support for this possibility comes from the deepest Chandra and XMM-Newton surveys which are most likely missing a significant fraction of the total AGN population. At least 50% of the $>6\ \text{keV}$ background is still unresolved and population synthesis models predict the sources of the unresolved X-ray background to be heavily obscured, so-called Compton-thick AGN ($N_{\text{H}} > 10^{24}\ \text{cm}^{-2}$). While there is a sizable population of Compton-thick AGN in the local Universe, their properties are basically unknown at larger distances. A population of Compton-thick AGN at redshifts around 2 may be hiding among infrared bright, optically faint galaxies. Even in the deepest Chandra fields few of them are detected individually, but their average hard X-ray flux corresponds to a hard X-ray luminosity $>10^{43}\ \text{erg s}^{-1}$, about one order of magnitude larger than the XEUS sensitivity limits. Individual detections and quite good quality X-ray spectra will be obtained by XEUS and will yield column densities, nuclear luminosities and ultimately the evolution of obscured accretion. By combining the capabilities of the XEUS HXI and WFI detectors, an almost complete census of the physical properties of Compton-thick objects will become possible over 90% of cosmic time. Fig. 3.2 shows a simulation of a deep survey, which clearly indicates XEUS's ability to detect and characterize the important source classes throughout the whole redshift range.

Feedback and downsizing

The fact that practically all galaxy bulges in the local Universe contain supermassive black holes, and the tight relation between black hole mass and, e.g. the stellar velocity dispersion point towards a physical connection and a co-evolution of stars and central black holes throughout the evolution of the Universe. Only recently has the importance of feedback from stellar explosions and accreting black holes into the intergalactic and interstellar medium, and thus its role in star and galaxy formation, been realized. Massive outflows from AGN are likely to be a crucial element in understanding the evolution of the baryonic components of the Universe (see e.g. Fig. 3.3). The most promising explanation for the correlation between black hole mass and host galaxy properties is that a strong wind from the AGN terminates the growth of stellar and black hole components by driving the interstellar

medium out into intergalactic space. XMM-Newton and Chandra have confirmed that ionized matter is common in nearby AGN, and have discovered that it is outflowing with velocities ranging from hundreds of km s^{-1} up to $0.1-0.2c$. Largely unknown, however, is the location of these winds, and thus the kinetic energy involved. The mass and kinetic luminosity of the outflows are predicted to be more prominent in X-rays than in the UV, thus requiring X-ray spectroscopy. XEUS will have the sensitivity and energy resolution not only to estimate the density and location of the outflows by studying time variability in nearby objects, but more importantly is also sensitive enough to characterize winds in "typical" QSOs at $z=1-3$, where the majority of galaxy growth occurs.

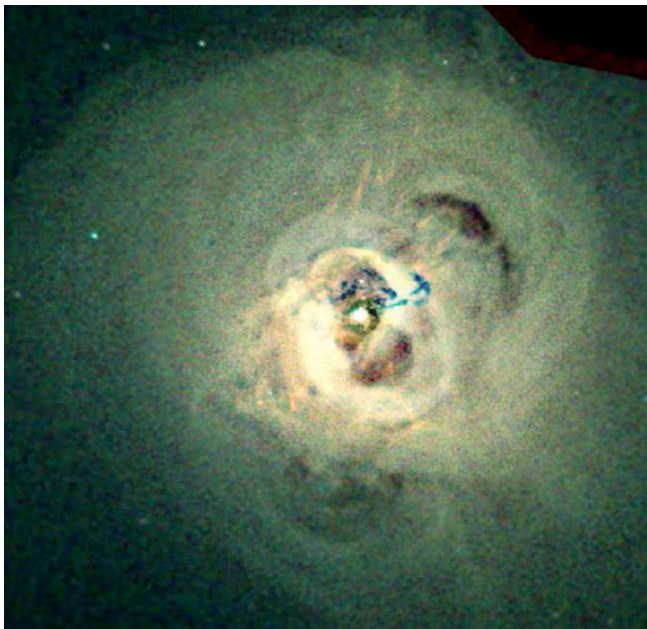


Figure 3.3 :Chandra observation (1 Ms) of the Perseus cluster, showing in detail the feedback of its central AGN to the surrounding. [3]

Recent observations at a wide range of wavelengths show compelling evidence that star formation and black hole growth shift to lower mass galaxies as the Universe evolves. This scenario is usually referred to as "cosmic downsizing", and must be related to the rapid decline in both the accretion and star formation histories of the universe since $z=1$. Deep X-ray surveys show that the space density of less luminous AGNs peaks at significantly lower redshifts than that of AGNs with high X-ray luminosities [4]. Studies in the nearby Universe suggest that this behaviour is driven by a decrease in the characteristic mass scale of actively accreting black holes. Strikingly similar behaviour has been found for the stellar population of galaxies, in that the stars in more massive galaxies are formed at higher redshift. This cosmological behaviour of the accretion history may be related to completely different channels for fuelling the central black hole: at high redshift, major mergers likely play the dominant feeding role. At lower redshift a more "gentle" mechanism has to be at work, which may be connected to "rebuilding" gas disks around spheroidal galaxies,

which could be the source of accreting material in Seyfert galaxies. Such a scenario predicts radically different properties for the nature of the AGN outflows (and hence spectra) in the two modes, which XEUS can easily distinguish.

The study of the AGN feedback on its host galaxy and surrounding environment will also receive a major boost by XEUS observations of radio sources. Inverse-Compton scattering of the CMB radiation field within a highly relativistic flow is commonly believed to explain the relatively strong X-ray emission detected with current X-ray instruments from large-scale quasar jets. This model is attractive because of its simplicity and energetic efficiency and it provides useful integrated constraints on the magnetic field strength and internal energy stored in powerful radio galaxy and quasar lobes. However, it faces significant challenges with the actually observed morphological properties of quasar X-ray jets, both in their multiwavelength and their redshift dependence. XEUS's massively increased sensitivity, together with the next generation radio facilities, LOFAR and SKA, will be able to clarify the basic model for the X-ray emission of radio galaxies and radio-loud quasars, thus answering long-standing questions about particle acceleration processes, particle and field content and their distribution. XEUS's hard-energy capability will enable X-ray spectral ageing analyses as a new probe of radio-source evolution and dynamics. By mapping group and cluster environments of radio sources to high redshift for the first time (see clusters science case), XEUS will also provide important new constraints on the epoch and environmental dependence of these radio-loud feedback processes.

X-ray redshifts: a new tool to characterise the universe

The study of iron emission lines from distant X-ray sources will take X-ray astronomy into a new era. Traditionally, X-ray surveys have relied upon painstaking followup work with other wavebands to determine redshifts and clarify the nature of the detected sources. The combined sensitivity, spectral resolution and bandpass of XEUS will, for the first time, allow redshift determination and source classification autonomously, based on the X-ray data alone. Examples are given in Figure 3.2, which shows clearly the ability of XEUS to determine redshifts out as high as $z\sim 7$, and to discriminate between unobscured QSOs, Compton thick AGN and thermal sources (e.g. groups, clusters and starbursts) based on the X-ray spectral properties alone. As discussed in section 3.3, XEUS is so power-

ful that it can even probe broad emission from the accretion disk out to high redshift. The study of iron line emission at very high ($z > 6$) redshifts also has important implications for the history of the metal production in the early Universe. The very detection of high redshift lines requires that iron has been quickly and efficiently produced by the explosions of the first supernovae possibly associated with a first generation of massive Pop III stars. XEUS observations will open up a new dimension of discovery space, providing an independent probe of the black hole and star formation history

3.2 Evolution of large scale structure and nucleosynthesis

The large scale structure of today's Universe is determined by the growth of dark matter density fluctuations, and by the dynamical action of dark matter and dark energy. The appearance is determined by the visible, baryonic matter embedded in the dark matter distribution. Significant progress has been made in constraining the cosmological parameters and in reconstructing the large-scale structure of the dark matter distribution, but we still lack an understanding of the evolution of the baryonic component of the Universe. Because of the complex behaviour of the baryonic matter, progress in our understanding is largely observationally driven. XEUS, combining very large collecting power with excellent energy resolution and good spatial resolution, is needed to directly observe the evolution of the baryonic matter in the warm/hot intergalactic medium (WHIM) and the hot plasma in galaxy clusters, and to trace galaxy evolution through the effects of energy release and nucleosynthesis. XEUS will be able to address major open questions like:

- Where are the missing baryons in the Universe, and what are the exact properties of the WHIM?
- What are the chemical and thermal properties of the first clusters?
- What is the physics and mass distribution of the evolving clusters?

Missing baryons and the WHIM

While baryons (~4% of the energy density) determine the visible appearance of the present universe (stars, galaxies, galaxy clusters, etc), about half of the baryons in the local Universe are unidentified, presumably constituting the WHIM with temperatures of 10^{5-7} K. This gas, photoionized by massive stars and active galaxies, has received additional heating during the formation of large-scale filaments, and has been enriched by heavy elements due to matter expelled from galaxies in early star-formation epochs. The WHIM is thus an important tracer of the large-scale structure and a reservoir of fossil heating and chemical enrichment generated by stars, galaxies and black holes throughout cosmic history. Due to the expected low density of the WHIM (10^{-5} – 10^{-6} cm⁻³) and hence low emission measure, absorption line spectroscopy against bright background objects is the most promising method of WHIM detection. Previous detections of OVI absorption lines in the UV continuum of bright AGNs account for only about 5% of the total baryonic matter, however, which indicates that the bulk of the WHIM must be in hotter gas visible only in the X-rays. X-ray measurements of redshifted OVII and OVIII lines have been reported for a number of AGN, but are of low significance and still controversial [5,6]. The photon collecting power of XEUS will be 300 times higher than that of the high-resolution spectrometers on Chandra and XMM-Newton. Thus a typical bright AGN ($F_X \sim 7 \times 10^{-12}$ erg cm⁻² s⁻¹) will yield a 4.3σ detection for OVII absorption lines with an equivalent width (EW) of 0.05 eV in a 150 ks XEUS NFI pointing. This sensitivity level, which can be achieved for about 80 sources in the sky, is factor of 50 smaller than the previously claimed results. Theoretical simulations predict a mean of 1.6 absorption features with EW 0.05 eV in the redshift range 0–0.3 for a random line of sight (for an O abundance of 0.1 solar). This way XEUS can probe the majority of the missing baryons in the local universe.

Physical properties of the first clusters

As discussed in 3.1, one of the most important revelations of recent XMM-Newton, Chandra and optical/IR studies, has been that galaxy feedback from supernovae and supermassive Black Holes (SMBH) must play a significant role, not only in the history of all massive galaxies, but also in the evolution of groups and clusters as a whole. These feedback mechanisms are likely to provide the extra energy required to keep the cluster centres from cooling all the way down to molecular clouds, to account for the entropy excess observed in the gas of groups and clusters, and to cure the overcooling problem and regulate star formation. It may also be responsible for the $M_{BH} - \sigma^*$ relation of Black Holes and their host galaxies as well as the loss of gas and thus the red sequence in elliptical galaxies. Feedback, e.g. via supernova (SN) driven galactic winds, also plays a central role in the chemical enrichment of the cluster gas and in the cosmic history of nucleosynthesis.

Various feedback processes, e.g. from SNe and SMBHs, as well as cooling, are expected to affect the intergalactic gas in different ways and on different time scales. The evolution of entropy and metallicity of the cluster gas, is the key information to disentangle and understand the relative role of these processes. One of the most important and most challenging goals of XEUS is thus to detect and study in detail the first groups and clusters in the redshift range $z=1.5-2$. To demonstrate the XEUS capabilities for determining the physical properties of the gas in distant, forming groups and clusters, we have performed detailed simulations (Fig. 3.4), including the important effects of the galactic foreground emission. Temperature, entropy and mass profiles (assuming hydrostatic equilibrium) will be measured for low mass systems up to $z=1$, with a precision currently achieved only for bright local objects. In addition, a large number of high redshift clusters, down to low mass groups ($kT=1$ keV) at $z=2$, will be detected serendipitously with the XEUS WFI (Fig. 3.4) and their spectral redshifts can be directly measured for fluxes as low as 10^{-15} erg cm^{-2} s^{-1} .

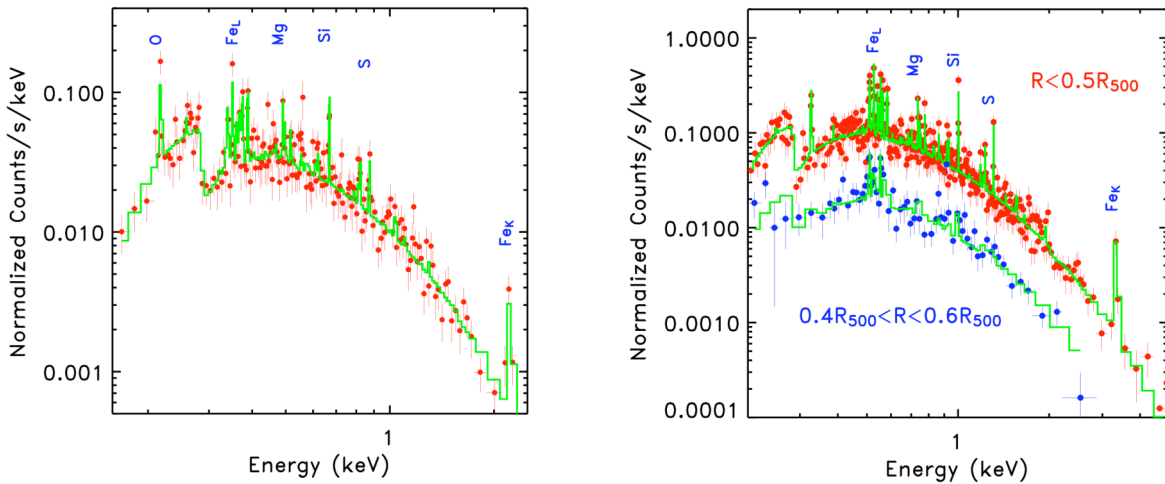


Fig. 3.4: Left: XEUS NFI 150 ks observation of a $kT=2$ keV, $z=2$ cluster with a bolometric luminosity of 7.7×10^{43} erg s^{-1} . The overall temperature and element abundances can be measured accurately: $\pm 2.8\%$ for kT , $\pm 30\%$ for O and Mg, $\pm 18\%$ for Si and $\pm 11\%$ for Fe. Right: The same cluster, but now at $z=1$, observed for 100 ks and for two extraction regions. In the $0.4R_{500}-0.6R_{500}$ annulus (R_{500} is a fiducial outer radius of the cluster where the mean cluster mass density is a factor of 500 above the cosmic critical density), the temperature and iron abundances are measured with an accuracy of $\pm 3.5\%$ and $\pm 20\%$ respectively (bottom spectrum), illustrating the capability of XEUS to measure temperature and abundance profiles at such redshift, even for low mass systems.

Physics and mass distribution of evolving clusters

The cluster mass and the dynamical structure are key properties in the use of galaxy clusters as cosmological probes and as laboratories for the cosmic evolution of the baryonic component. XEUS, via detailed spatially resolved X-ray line spectroscopy and hard X-ray imaging, will determine the multi-temperature structure of the intracluster medium (ICM), the dynamics of the ICM, and the nature of particle acceleration in clusters. Present cluster mass determinations are hampered by (i) the inability to distinguish a mixture of temperatures from a single temperature (the spectroscopic results for the mixture are generally biased towards low temperatures) leading to significant errors in the mass determination, and (ii) our ignorance of the dynamical pressure of gas motions in the cluster ICM. Both problems can be tackled by XEUS high-resolution spectroscopy in regions of nearby clusters and in deeper exposures of distant clusters. For a typical cluster region with a flux of 5×10^{-13} erg s^{-1} cm^{-2} (0.5–2 keV), different temperature components in hot clusters (4–8 keV) can be separated with a precision of about 0.3 keV in a 150 ks NFI observation; at lower temperatures the spectroscopy becomes even easier. For the same X-ray flux, the expected velocity broadening in the range of 200–600 km s^{-1} in cooling core and post-merger clusters, can be measured in the iron lines with an accuracy of several 10 km s^{-1} , sufficient to estimate the dynamical pressure in clusters for the expected velocity (see Fig. 3.5). The line width measurement provides an integral measure of internal dynamical pressure of the ICM (turbulence) which should be accounted for in the mass measurement. Another important dynamical ICM component is the relativistic plasma seen through radio synchrotron emission in merging clusters and in AGN-ICM interaction regions. The mapping of inverse Compton emission from this plasma, so far not even clearly detected, will definitely be possible with XEUS providing important information on the energy density and magnetic fields in this plasma component. The XEUS observations will thus greatly help to understand cluster masses, the process of cluster mergers, the frequency of cluster mergers reflecting their cosmic evolution and the heating processes in cooling cores.

The formation of structure in the universe reflects the action of dark matter and dark energy. Galaxy clusters are crucial tracers of this large-scale structure, and hence XEUS can probe the nature of the dark sector via observa-

tions of clusters and their evolution. XEUS will greatly improve constraints on the parameters describing the nature of dark energy with galaxy cluster surveys, and by using galaxy clusters as standard candles by means of the Sunyaev-Zeldovich effect and the universal baryon fraction of the cluster mass. Numerical simulations of galaxy cluster formation have reached a stage where realistic modelling including all hydrodynamical and galaxy formation feedback processes have become feasible. The appropriate physics of these processes is not always clear, such as the importance of heat conduction and viscosity. But these aspects can be calibrated by a detailed comparison of observations and simulations. XEUS will provide, for the first time, the details for a sufficiently critical comparison. We expect that the major breakthrough of a detailed understanding of cluster formation, cluster structure, mass determination, and chemical abundance measurements will come from simulation-assisted interpretation and modelling of observational data. A better understanding of the baryonic physics in clusters will remove the major systematic uncertainties in the utilization of X-ray clusters for precision cosmology and the study of dark energy.

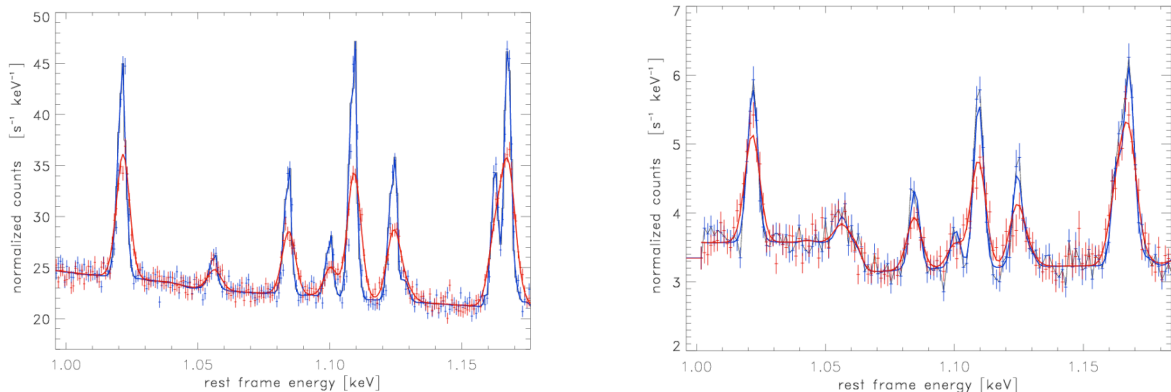


Fig. 3.5: XEUS NFI spectra around the Fe L-line complex. Left: an emission region in a cluster with $F_x(0.5\text{--}2\text{keV}) = 10^{-13} \text{ erg cm}^{-2} \text{ s}^{-1}$ at $z=0.2$. Right: a cluster with $F_x=1.5 \times 10^{-14} \text{ erg cm}^{-2} \text{ s}^{-1}$ at $z=1$. In both cases a velocity broadening of the lines by 100 (blue) and 600 km s^{-1} (red) has been assumed. The velocities can be determined with an accuracy better than 10 km/s in the nearby cluster in a 100 ks observation and with an uncertainty of $\sim 20\text{--}50 \text{ km s}^{-1}$ for the distant cluster in a 250 ks observation.

3.3 Matter under extreme conditions

The most extreme physical conditions in the observable Universe, regions with strongest gravity, highest densities, hottest temperatures and largest magnetic fields, occur around black holes and neutron stars. They are responsible for the most dramatic events and powerful sources known, and test physics and astrophysics to the limit. Understanding how strong gravity works and testing our understanding of General Relativity (GR) requires observations of matter and radiation in regions just outside the event horizon of black holes. The extreme gravity there produces large Doppler shifts, gravitational redshifts and light bending, as well as frame dragging if the central mass is rotating. Studies of the accretion flow around and upon the surfaces of neutron stars provide constraints on the strong interaction and thus the equation of state of nuclear matter. All these effects can be seen or inferred from the X-ray spectra and variability of accreting black holes and neutron stars, since X-rays are a major component of the radiation from the innermost parts of accretion flows and compact surfaces. XEUS will address the major open questions like:

- How does gravity in the strong field limit work and what are the properties of curved spacetime?
- What is the geometry of accretion flows around black holes and neutron stars?
- What is the equation of state of nuclear matter?

Strong gravity

The accretion flow in luminous sources consists of an optically thick accretion disc generating quasi-blackbody radiation with a coronal region above and below it. Comptonization in the corona of soft photons from the disc produces a power-law X-ray continuum which in turn irradiates the disc giving rise to a reflection spectrum, consisting of backscattered continuum with superposed fluorescent and recombination lines. The reflection spectrum has a characteristic shape and is commonly seen in accreting sources. As discussed in 3.1, emission lines, particularly from iron in the 6.4–6.9 keV band, enable redshifts to be determined. In accreting black holes the whole reflection spectrum is relativistically broadened. Measurements of the degree of broadening then translate into values of the innermost radius of the disc and thus, through the effects of frame dragging on the innermost stable orbit, into the determination of the spin of the black hole.

An astrophysical black hole is characterized by just its mass and spin. Mass can be measured at large radii but spin requires a probe, such as an accretion disc or a blob, at small radii. The degree of spin depends on the accretion and merger history of the black hole. X-ray observations of the AGN MCG–6–30–15 in Fig. 3.6 (left) indicate that it has a high spin close to the maximal Kerr value. The strength of the reflection component relative to the direct power-law continuum depends on the geometry of the inner disc and corona and on the degree of light bending. It is so strong in some AGN that significant light bending is inferred to take place, as expected from the bending of spacetime so close to a black hole. Studies of the strong gravity effects are now beginning to reveal the geometry and behaviour of the inner regions of accretion flows around black holes within a few times the radius of the event horizon. Electron scattering of the X-ray photons, which produces both the power-law continuum through Comptonization and the reflection continuum, is intrinsically polarization dependent. Thus the continuum should be polarized by 5–15%, at angles which depend on the geometry of the emission region, the relative amounts of direct and reflected radiation and on propagation in curved spacetime.

XEUS has the potential to readily observe all these effects in accreting black holes, both stellar mass ones in binary systems (Galactic Black Holes, GBH) and the SMBH in galactic nuclei. AGN give the highest count rate per orbital period of the innermost regions, so are optimal for observing individual variations of the flow in the relativistic regime. Such variations can be deduced in a statistical sense from the GBH. The flow is turbulent so transient orbiting blobs are expected. Mapping their behaviour and measuring orbits over a range of radii will give a check on GR in the extreme regime. Current observations, with e.g. XMM-Newton, indicate that such variations occur but cannot quantify them well. The much larger collecting area of XEUS will easily open up this crucial area for detailed study (Fig. 3.7), and the high spectral resolution of the NFI can trivially deconvolve narrow components, as well as a complete determination of the effects of complex absorption.

Several hundred bright, nearby AGN can thereby be studied on timescales comparable to the inner orbital times, enabling the behaviour at different black hole masses and accretion rates to be explored, but the real interest is in how this might change at high redshift. Chandra and XMM-Newton deep surveys have already pushed Fe-line profile studies of this kind to cosmological distances. The average rest-frame spectrum of a large number of

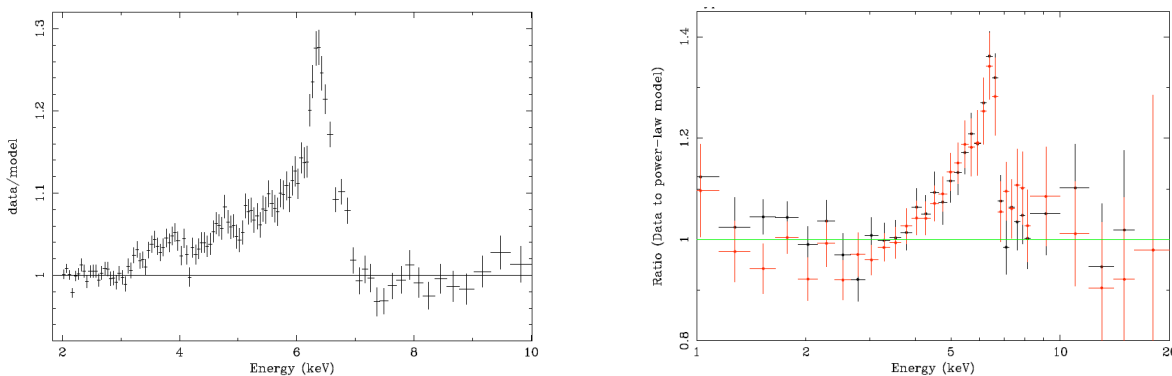


Figure 3.6: Left: The broad iron line in MCG–6–30–15 from an XMM observation [7] shown as a ratio to the continuum model. Right: Similar plot for the mean spectrum of type-1 AGN in the Lockman Hole [8]. XEUS will deliver data of similar quality to MCG–6–30–15 for individual AGN at cosmologically interesting distances ($z \sim 1$) and may even detect broad emission out to $z \sim 7$ see Fig. 3.2).

moderate to high redshift AGN detected in XMM-Newton and Chandra deep surveys shows evidence for the presence of a prominent red wing in the line profile, most likely due to strong GR effects close to a rotating SMBH (Fig. 3.6 right). This is very good news for XEUS, because it demonstrates that broad iron lines will be routinely detected in deep pointings in many sources contributing to the X-ray background, thus promising a wealth of Fe-line diagnostics. Whether the red wing is associated with a rapidly spinning Kerr BH and how its intensity and shape depend on the source properties (redshift, luminosity, obscuration, etc.) is the subject of an active debate requiring more sensitive X-ray observations. In particular the study of the line profile over a broad range of redshifts and luminosities will provide unique information on the evolution of black hole spin over cosmic time.

Closer to home, the time-averaged properties of GBH in our own and nearby galaxies can be observed and compared with those of AGN to better understand how accretion operates onto black holes over the whole mass range from 5 to billions of Solar mass. GBH also make very large luminosity excursions (transient sources and state changes) which will stretch and test our comprehension of the physical processes and assumptions. If, for example, the same spin parameter is found from observations of an object over a wide range of conditions and orbital radii then we can build confidence in our understanding and in the underlying physical principles, including GR.

X-ray QPOs probe the orbital motion of matter under extreme conditions of gravity, temperatures (up to 10^9 K) and velocities ($0.5c$). Although we currently lack a unanimously accepted model for high frequency QPOs, which are seen both in NSs and BHs, most models associate the QPOs with GR frequencies. XEUS/HTRS will be more than ten times more sensitive than RXTE (up to at least 25 keV). This will open the way to detect strong QPOs on timescales closer to the coherence time of the underlying oscillator, and detect the weakest features predicted in models. This will remove the degeneracy in their identification and detect QPOs in fainter and more distant

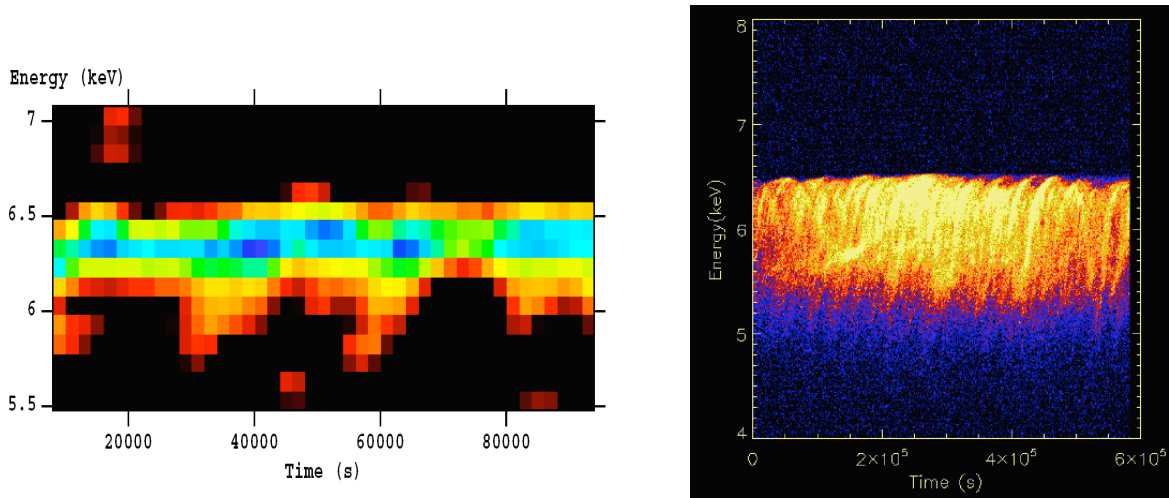


Figure 3.7 Left: Excess iron line emission versus time in an XMM-Newton observation of NGC3516 showing tentative evidence for orbital motion at $\sim 10 r_g$ around the black hole [9]. Right: Simulated XEUS energy-time map for iron lines from a turbulent disc around a black hole [10].

sources, such as the still puzzling ultra-luminous X-ray sources which may contain intermediate mass BHs. In the XEUS era, the theoretical understanding of accretion disk physics as well as global disk simulations will advance. This will provide the necessary framework for exploiting the great potential of QPOs to probe GR in the strong field regime, to constrain the mass, radius, and spin of compact objects over a complete set of accreting systems from cataclysmic variables to super massive black holes in AGNs. More generally, fast X-ray timing probes accretion disk physics on the dynamical timescales of the inner parts of the flow, providing complementary measurements of the quantities also probed by X-ray spectroscopy (e.g. the spin with the broad iron lines). In addition, when combined with polarimetry, it enables us to constrain the accretion geometry and emission processes at work in accreting binaries, and study the coupling between accretion and ejection in relativistic jet sources (microquasars, gamma-ray bursts). Moreover the joint use of the complementary capability of XEUS and LOFAR (LOw Frequency ARray) – the first radio telescope able to trigger on radio transients – will provide a new outlook on the field of X-ray/radio transients.

Extreme physics

In Neutron Stars (NSs) the density in the core can be several times nuclear. Similarly, the magnetic fields can exceed by ten orders of magnitude the strongest fields generated in terrestrial laboratories. Hyperon-dominated matter, deconfined quark matter, superfluidity, even superconductivity are predicted in NSs. Similarly, quantum electrodynamics predicts that in strong magnetic fields the vacuum becomes birefringent. This makes NSs ideal laboratories not only for astrophysics, but also for nuclear and particle physics.

Different Equations of State (EoS) predict different maximum masses and mass-radius relations. Determining the EoS requires measuring the mass (M) and radius (R) of the NSs simultaneously. So far the most accurate mass measurements have been for binary radio pulsars. All measures cluster around the canonical $1.4 M_{\text{sun}}$, a value which can be accommodated by virtually all EoS. XEUS, by combining for the first time a high count rate instrument (HTRS) capable of coping with a few million events per second, together with improved spectral capabilities in X-rays (WFI, HTRS & TES) will probe NS radii and hence determine the physical state of matter in its densest form found in the observable Universe.

A statistically significant sample of NSs will be observable over a wide range of luminosities, from the dimmest states up to the brightest states during Eddington limited X-ray bursts. XEUS can sample a wide range of ages (from birth to 10^{10} years), and a variety of conditions, with the NSs being powered either by accretion, nuclear energy, internal heat release, or magnetic energy. X-rays alone provide several complementary diagnostics for the same object. For the EoS, these diagnostics include (i) X-ray burst spectroscopy, enabling us to detect gravi-

tationally redshifted emission lines and absorption edges, (ii) waveform fitting of X-ray pulsations produced by rotating hot spots, either during X-ray bursts or in the persistent emission of pulsars, (iii) X-ray spectroscopy of cooling NSs and measurements of the associated cooling curves whose shape depends on the NS structure and internal composition, iv) the study of the sub-ms variability from the innermost regions of accretion disks (high frequency quasi-periodic oscillations, QPOs, recently discovered by the Rossi X-ray Timing Explorer, RXTE) and v) the detection of kilo-Hz seismic vibrations in magnetars after giant flares.

While obtaining such diagnostics, nuclear burning will also be probed and the properties of NS atmospheres, which depend on the magnetic field, will be measured. Similarly XEUS will estimate the spin frequency distribution of NSs spun up by accretion and test the exciting hypothesis that the distribution is bound below 750 Hz, due to angular momentum losses via gravitational radiation. Magnetic fields will be measured directly with X-ray spectroscopy through the unambiguous detection and identification of cyclotron resonance scattering features, as well as through its unique polarimetric signatures. X-ray polarimetry will address the origin and the structure of the magnetic field, and its role in the cooling of NSs. In addition, the vacuum polarization in magnetic NSs will be detectable, as it is expected to alter significantly the surface emission and induce clear polarization signatures in X-rays.

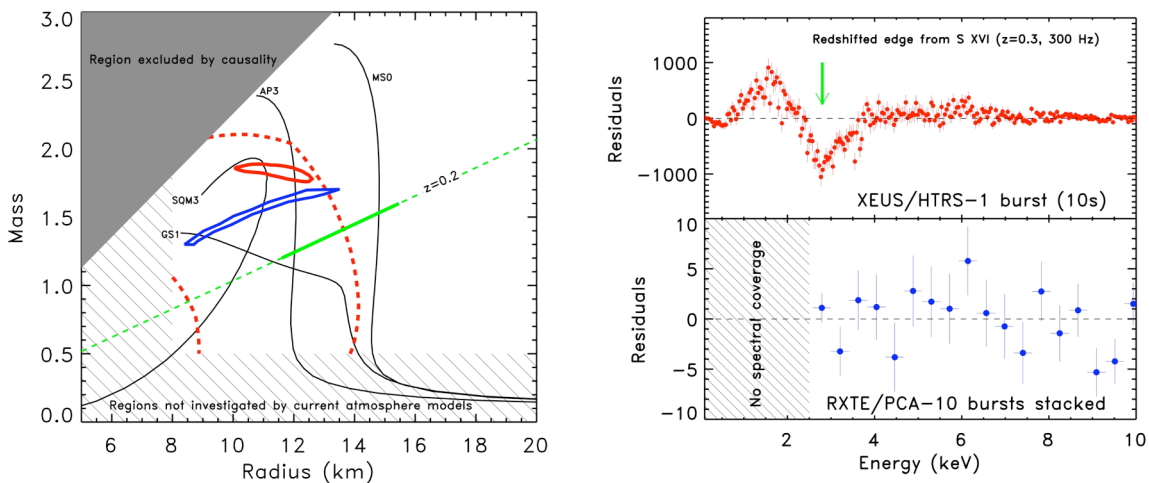


Fig. 3.8: Left: Mass-radius relations for representative EoS involving standard nucleonic matter (AP3 and MS0), strange quark matter (SQM3), Kaon condensates (GS1). For illustrative purposes, the constraints derived from XEUS are from (i) a gravitational redshift ($z=0.2$) for a source for which mass function is known (green bold solid and dashed lines), (ii) waveform fitting of pulsations obtained from a 2 hr observation of an accreting millisecond pulsar (blue contours), (iii) hydrogen atmosphere model fitting of the X-ray spectrum of a quiescent NS in the globular cluster Omega Cen (red contours, 99%). The best available constraints from XMM-Newton to date for the same object are also shown (red dashed line) to illustrate the gain provided by XEUS. Right: A comparison between XEUS/HTRS and RXTE/PCA for the detection of a photoionization edge predicted ($E_{\text{QW}}=300$ eV) from S XVI ashes left after one X-ray burst (smearing due to rotation at 300 Hz taken into account).

As illustrative examples of breakthroughs expected with XEUS, Fig. 3.8 shows the constraints on M and R set by the three different methods discussed above. Combining these diagnostics from many NSs will pinpoint the correct EoS. Such measurements are only possible with XEUS, because XMM-Newton, Chandra and Suzaku are unable to cope with count rates of up to 10^6 cts s^{-1} , typical for X-ray bursts and accreting pulsars, whereas RXTE/PCA has insufficient spectral resolution.

3.4 Dynamics and chemistry of cosmic plasmas

Hot cosmic plasmas emit mostly at X-ray wavelengths and an observatory like XEUS will provide a unique opportunity to study their dynamics and chemical abundances in various conditions as those occurring in accretion disks, SN, SNR, Stellar Coronae & Winds, Clusters, etc. The following selected key scientific issues exemplify XEUS' unique role as an observatory with a wide-ranging appeal.

Stellar evolution, plasma physics and feedback into the interstellar medium

Stellar X-ray emission deeply affects the formation and evolution of stellar and planetary systems as well as the origin and acceleration of stellar wind and mass loss. Those high-energy phenomena provide examples of physical processes that occur on much larger scales in distant cosmic X-ray sources and offer "nearby" laboratories for an advanced understanding of the basic plasma processes at work.

Understanding the high-energy ionizing emission of young low-mass stars, as revealed by Chandra and XMM-Newton is crucial as it can provide the way to couple the star and its accretion disk (via magnetic fields), to ionize its surface, and to influence its chemistry. Young Stellar Objects (YSOs) are luminous X-ray emitters; yet, embedded very young nearby YSOs have failed to be detected to much lower limits. The XEUS WFI will have adequate sensitivity to detect highly absorbed X-rays and to study their effect on the star formation process.

Line shifts and broadening in Chandra spectra of the very active late-type star AB Dor allowed a glimpse on the spatial structure of the X-ray emitting plasma [11]. Observations of the FeXXV, S, Si and Mg lines with the XEUS NFI, with its combination of high throughput, spectral resolution and time coverage, can provide us with a full Doppler image. Similar imaging of chromospherically active T Tauri stars will for the first time localize the X-ray emitting region to look for the long predicted magnetically confined, X-ray active channels, which should connect the stellar surface and the accretion disk.

With their short lifetimes and their mechanical and chemical feed-back into the ISM, through their powerful stellar winds and SN explosions, early-type OB and Wolf-Rayet stars are the actual drivers of the ecology of galaxies. With the XEUS NFI, we will for the first time be able to collect high-resolution high-quality spectra of a significant sample of these stars, allowing detailed studies of the profiles and of the temporal variations of the lines. These spectra will likely establish the importance of magnetic fields in early-type stars and eventually realize the long-held promise of X-ray spectroscopy to accurately measure the chemical composition of the winds of objects in various evolutionary stages.

Supernovae and their remnants

The study of supernovae and supernova remnants is important for understanding chemical enrichment in the Universe. In core collapse SNe, a massive star implodes into a neutron star, or black hole, while in the thermonuclear SNe, or Type Ia SNe, a C/O white dwarf disrupts after accreting enough mass from a companion so that in its centre the C/O combusts. For SNe, X-ray emission is mostly coming from core collapse SNe of stars surrounded by a dense circumstellar wind. The interaction with this material leads to shock formation, both heating the wind material and the SN ejecta. As the reverse shock evolves, and the material becomes optically thin at X-rays, progressively the shock lights up deeper and deeper layers of the SN. Typical SNe are too faint for high resolution spectroscopy with current observatories, which could disentangle the rich, superimposed spectra of different layers. XEUS will revolutionize these studies, having both the high spectral resolution and the effective area to obtain high signal to noise spatial resolved spectra.

For SNRs, X-ray emission is crucial to study the composition of the shock-heated material. For young remnants the dominant emission comes from the ejecta, made of material synthesized during the life of the progenitor and, for the innermost regions, during the explosion itself. The spatial distribution is also important, as it contains information about the dynamics of the explosion. For example, two models for Type Ia explosions, deflagration and delayed detonation, give roughly the same ejecta composition, but for the delayed detonation, the material from different layers is much more mixed. Moreover, evidence is emerging that the explosion mechanism for core collapse SNe is complicated and may require bi-polar explosions, which may be linked to the most extreme bi-polar SNe: gamma-ray bursts.

In collision-less supernova remnant (SNR) shock heating is likely released through plasma waves, but the detailed mechanism is poorly understood. The SNR shocks are thought to be the site of efficient acceleration and the dominant contributors to cosmic rays, at least up to energies of $\sim 10^{15}$ eV. However, the energy budget of shocks and, in particular, the fractions of energy going into plasma heating and cosmic ray acceleration are poorly known. If the cosmic ray acceleration is very efficient, the shock compression ratio will be higher, and the plasma temperature lower. With CCD spectra we can determine the electron temperature from the continuum and line ratios, while the temperature for protons and other ions requires the measurement of thermal Doppler broadening utilizing spatially resolved, high resolution spectroscopy enabled by the XEUS NFI. For a shock velocity of 4000 km s^{-1} one expects an OVII line broadening of 7 eV (FWHM). By the time XEUS is in orbit it is also likely that the Cherenkov Telescope Array (CTA), a sensitive new TeV gamma-ray telescope, will be at work. Combining electron and ion temperatures derived with XEUS with cosmic ray energies derived with CTA will allow the measurements of the energy budget of SNR.

Galactic centre and tidal disruptions

The ignition and evolution of supermassive black holes in Galactic Nuclei is most likely a transient, possibly recurrent, phenomenon with typical timescales of the order of 10^7 years. An intermediate case is the tidal capture, dis-

ruption and successive accretion of individual stars expected to happen every 10^{4-5} years in the center of a normal galaxy. Highly accreting black holes are bound to end up in a quiescent state at later times. Sgr A*, the supermassive Black Hole in the Galactic Centre, is the best known example. It is extremely quiet, accreting at about 10^{-7} of the Eddington luminosity, but with frequent X-ray flares. The outbursts are up to 100 times brighter than the quiescent emission and are believed to originate within a few Schwarzschild radii. At a distance of 8 kpc, Sgr A* is an ideal laboratory to study accretion processes at low rates, and to probe strong gravity effects. The presence of X-ray Reflection Nebulae (XRN) in the neighbourhood suggests that it was as active as a low luminosity AGN just a few hundreds years ago. The XEUS polarimetric capability will test this hypothesis, because the polarization angle of the reflected (and therefore highly polarized) radiation must be at 90 degrees with respect to the direction of the illuminating photons. In addition, the unprecedented XEUS throughput will allow to search for XRN and tidal capture flares in nearby galaxies, addressing the issue of the duty cycle of activity in normally inactive galaxies.

3.5 Requirements on the proposed payload

To meet the science aims discussed above, a suite of focal plane instruments in conjunction with a high-throughput grazing incidence X-ray mirror system is proposed (see section 5). The requirements imposed on this instrument complement are summarized in Table 3.1.

Table 3.1: Science Requirements on the Payload

PARAMETER	REQUIREMENT (GOAL)	SCIENCE DRIVER
Effective area (m ²)	1 (1.5) @ 0.2 keV 5 @ 1 keV 2 @ 7 keV 1 @ 10 keV (0.1) @ 30 keV	WHIM, early BHs, clusters Clusters, WHIM, early BHs EOS, gravity in strong fields EOS, acceleration, early BHs Acceleration, early BHs, EOS
Energy range (keV)	0.1–40	BHs, acceleration, clusters
Angular resolution (arc-sec)	5 (2) @ < 10 keV 10 @ 40 keV	Clusters, early BHs, WHIM Early BHs
Field of view (arc-min)	7 (10) diameter: WFI, HXI 1.7 diameter: NFI	Clusters, early BHs, acceleration Clusters, enrichment, galaxy evolution
Spectral resolution (eV)(FWHM)	2 (1) @ 0.5 keV: NFI 2 @ <2 keV: NFI 6 (3) @ 6 keV: NFI 150 @ 6 keV: WFI 1000 @ 40 keV: HXI	WHIM Clusters Clusters, enrichment, galaxy evolution Early BHs Early BHs
Point source detection sensitivity, erg cm ⁻² s ⁻¹	(3 x 10 ⁻¹⁸) @ 0.2–8 keV; 4σ	Early BHs
Time Resolution (s)	10 ⁻⁵ : HTRS	EOS studies
Count rate capability (s ⁻¹)	2 10 ⁶ : HTRS	EOS studies
Polarimetry (MDP, 3σ-confidence in 10 ks)	2% at 10 ⁻² Crab: XPOL	EOS studies
Observing constraints	>2 weeks visibility each 6m ToO response in (<1 day) 10 ³ (5.10 ⁴) s cont. observ. ±5° (±15°) range Sun angle	EOS studies EOS studies EOS studies, strong gravity EOS studies

4 Mission profile

XEUS comprises both a Mirror SpaceCraft (MSC) and a Detector SpaceCraft (DSC). The MSC contains the X-ray optics and the DSC the prime focal plane instruments. The instruments will be kept at the primary focus of the X-ray optics (one at a time) using the concept of formation flying.

4.1 Launcher requirements

The two spacecraft will be launched together in a single stack on the Ariane 5 ECA. The XEUS MSC, containing the mirror with its outer diameter of 4.2m, fits in the 4.57m diameter of the Ariane 5 ECA fairing. The inner diameter of the mirror is compatible with the adapter 1194H. The DSC will be mounted on the top of the MSC. With non-deployable baffles, the spacecraft stack fits in the length of the medium fairing (Fig. 4.1). In this configuration the launcher can place both spacecraft at L2 using a direct launch and with a total wet mass of 6.5 tonnes.

4.2 Orbit requirements

A Halo orbit around the second Lagrangian point of the Sun-Earth system (L2) is selected as providing optimal conditions with respect to perturbations, stable thermal environment, lack of eclipses, and sky visibility. The orbit is eclipse-free for 5+ years, and can be reached by free-transfer in about one month for an almost full-year launch window. The L2 location provides the necessary low gravity-gradient environment for economical formation flying, long observing windows and optimal cooling for the instruments. XEUS can build on the L2 halo experience of Herschel, Gaia and JWST. The present baseline is to fly as a single composite (DSC+MSC) and to separate only after completion of all major orbit manoeuvres (Fig. 4.2)

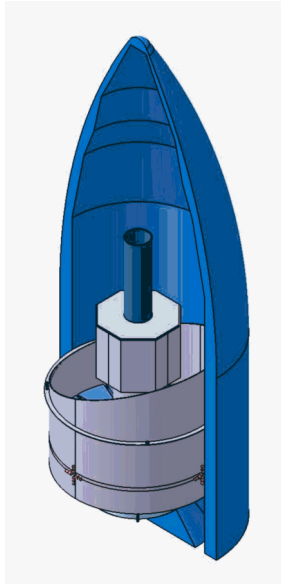
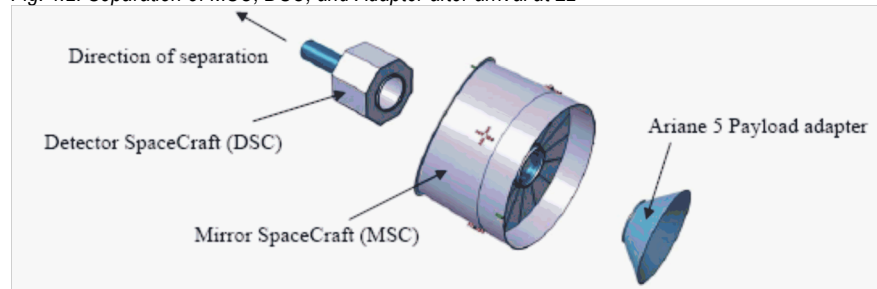


Fig. 4.1: DSC on top of MSC inside Ariane medium fairing

Fig. 4.2: Separation of MSC, DSC, and Adapter after arrival at L2



4.3 Ground segment requirements

The two spacecraft will be tracked from ESA ground stations and mission operations will be conducted by ESOC as for XMM-Newton. Special attention needs to be given to optimising formation-flying resources at ESOC. Science operations will be conducted by the XEUS-SOC as elaborated in section 7.

4.4 Special requirements

XEUS will be operated at L2 and therefore there will be a cruise phase prior to spacecraft separation and the establishment of formation flying. During the main mission phase the acquisition of targets and conduct of observations will require simultaneous operations with MSC and DSC. Critical issues are discussed in later sections.

5 Instrument payload

5.1 Model payload

The science aims of XEUS (Tab. 3.1) are very demanding and require state of the art instrumentation. First of all a single X-ray mirror of at least 5 m² effective area at 1 keV with a spatial resolution < 5 arcsec (goal 2 arcsec), and a focal length of 35 m is required. The focal plane plate scale for this optic equals 170 μm/arc-sec. Furthermore the requirements on spatial resolution, FoV, energy resolution, energy range, quantum efficiency, count rate capability, and polarization sensitivity cannot be met by a single focal plane instrument. Therefore the following instrument complement (Tab. 5.1) in the focal plane of the optic, is proposed for the model payload to meet the science objectives:

- A wide field imager (WFI) covering the 0.05–20 keV energy range with large FoV, excellent spatial resolution and efficiency, good energy resolution, and adequate count rate capability
- A confocal hard X-ray imager (HXI) that covers the same FoV with excellent spatial resolution and efficiency in the 10–40 keV energy range, in combination with good energy resolution and count rate performance
- A high spectral resolution imager (NFI) that covers the 0.1–20 keV energy range with unprecedented energy resolution, narrow FoV and relatively low count rate capability
- A non-imaging high time resolution spectrometer (HTRS) that covers the 0.1–20 keV energy range with good energy resolution but ultra-high count rate capability
- An imaging X-ray polarimeter (XPOL) with a narrow FoV, modest energy resolution, and excellent sensitivity to polarization in the 1.9–6 keV energy range.

Table 5.1: Performance and technical characteristics of the proposed payload. The performance characteristics have to be compared with the science requirements in Tab. 3.1.

Characteristics	WFI	HXI	NFI	HTRS	XPOL
Detector Type	Silicon active pixel sensor	CdTe and Si strip detectors	TES micro-calorimeter	Silicon drift detector	Gas pixel detector
Pixel size (μm^2)	75 x 75	220 x 220	240 x 240; 490 x 490	2.500 \emptyset	50 x 50
Number of pixels	1.000.000	640 CdTe strips 1280 DSSD strips	1.024 (240) ; 768 (490)	19	105600
Array size (mm^2)	76 x 76	70 x 70	16 x 16	15 \emptyset	15 x 15
Field of view (arc-min^2)	7.6 x 7.6	7 x 7	1.6 x 1.6	1.5 \emptyset , no imaging	1.5 x 1.5
Energy Range (keV)	0.1–20	10–40	0.1–20	0.1–20	1.9–6 ⁱ
Energy Resolution (eV)	40 @ 0.3 keV 125 @ 6 keV	< 1 keV	2 and 4 @ 2 keV ⁱⁱ 5 @ 6 keV	50 @ 0.3 keV 150 @ 6 keV	700 @ 2 keV 1200 @ 6 keV
Non X-ray detector background in counts.($\text{cm}^2.\text{keV.s}$) ⁻¹	5×10^{-3} ⁱⁱⁱ	5×10^{-4} (derived from in orbit Suzaku data)	5×10^{-3} (derived from XRS/Suzaku)	Not relevant	2.5×10^{-3}
Countrate/pixel/s with 10% pile-up	100 (Full-Frame)	20.000 TBC	75; 25	> 100.000	20.000
Countrate/source/s with 10% pile-up (5" telescope)	6000 (Full Frame)	20.000 TBC	1500; 200	> 2.000.000 (5 Crab)	20.000
Timing accuracy (μs)	1 ms(FF) 10 μs (PF)	10	10	10	10
Typical/Max telemetry (kbits/s)	typ. 45 max. 500	typ 10 max. 1000	typ 3 max. 360	Typ 50 Max < 1000	typ. 15 max.1500
Sensor temperature (K)	210	230–250	50×10^{-3}	250	260
Thermal load (W)	20	2	2 – 5 μW @ 50 mK	1	0.5
Type of Coolers	radiator + Peltier	radiator + Peltier	radiators + closed cycle coolers + ADR	Radiator+Peltier	radiator + Peltier
Cooler mass (kg)	10	1	300 incl. 40 for cryostat	0.5	1.0
Cooler power (W)	Max. 20	2	600	1	1
Baffle size (m)	7.9 x 1 diameter	Baffle of WFI + multilayer	2.8 x 0.36 \emptyset	0.3	2.8 x 0.36 \emptyset
Baffle mass (kg)	107 (structural element)	+ 31 (incl. skirt)	8	0.5	8
Instrument mass, excl coolers (kg)	70	38	50	22	14.3
Instrum. power (W) ^{iv}	240	44	212	70	33
Total mass (kg)	187	70	358	23	23.3
Total power (W)	260	46	812	71	34

This brings the total instrument mass at the DSC to 661 kg and the power to 1223 W.

ⁱ Efficiency > 2% and modulation > 10%

ⁱⁱ For small and large pixels, respectively

ⁱⁱⁱ EPIC-MOS on XMM has a background of 3.4×10^{-3} counts. $\text{cm}^{-2}.\text{keV}^{-1}.\text{s}^{-1}$

^{iv} including 70% DC-DC efficiency, excluding coolers

5.2 Sensitivity Calculation

Depending on energy and instrument, the XEUS effective photon collecting area (throughput) is about a factor of 40–50 larger than that of the XMM-Newton low-resolution spectrometric imagers (pn & MOS) and several hundred times larger than that of the XMM-Newton reflection grating (Fig. 5.4).

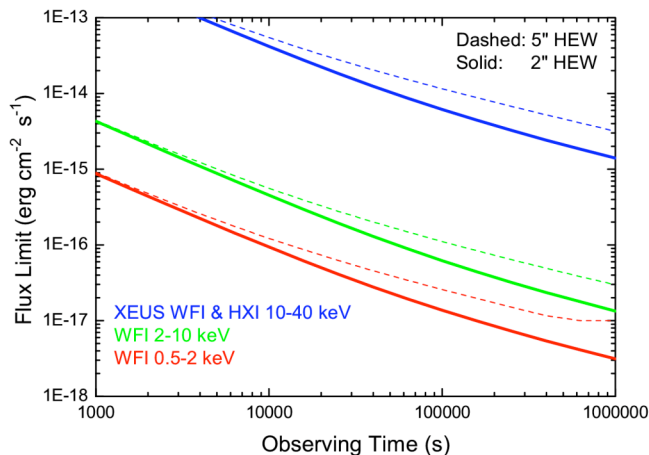


Figure 5.1: XEUS WFI & HXI sensitivity as a function of observing time for different energy bands. The requirement (5'', dashed) and goal (2'', solid-) angular resolution have been assumed for all cases. For the lower angular resolution cases, the sensitivity degrades due to the higher background and ultimately in the 0.5-2 keV band due to the source confusion limit.

LEGS results [12]. The unresolved extragalactic (mainly AGN) component is assumed to be 20% of the hard diffuse X-ray power-law component $10 E^{-1.42} \text{ ph cm}^{-2} \text{ s}^{-1} \text{ keV}^{-1} \text{ sr}^{-1}$. This fraction is somewhat arbitrary, as it depends on sensitivity, but it is probably conservative. In particular below 1 keV, the excellent energy resolution of the NFI gives a significant advantage, since source emission can be detected in between the “sky lines” of the Galactic foreground.

Combining the telescope throughput with the modelled background rates we can calculate the expected sensitivity for different energy bands as a function of observing time, which is shown in Fig. 5.1. Depending on the resolution of the telescope, we obviously arrive at different sensitivities. The final sensitivity limit is set by source confusion, which we assume to become important below 40 beams per source. Here we define the beam size as the half-energy width (HEW) of the point-spread-function (PSF).

5.3 Key characteristics of instruments

X-ray optics

The XEUS mirror is the heart of the XEUS mission and its challenging requirements (Tab. 5.2) call for the development of new technology. NASA's Chandra Observatory has an angular resolution of 0.5 arcsec with a collecting area of only $\sim 400 \text{ cm}^2$ at 1 keV and an area-to-mass ratio of $\sim 0.8 \text{ cm}^2/\text{kg}$. ESA's XMM-Newton Observatory consists of 3 identical mirror systems with each $\sim 1400 \text{ cm}^2$ at 1 keV with a modest angular resolution of ~ 15 arcsec and an area-to-mass ratio of $\sim 6 \text{ cm}^2/\text{kg}$. The huge area required for XEUS and the limits set on mass by affordable launchers require development of optics with an area-to-mass ratio of about $35 \text{ cm}^2/\text{kg}$. So the challenge is to produce a mirror system with a significantly larger area to mass ratio than provided by current technology, while at the same time retaining a high angular resolution. Using reflection at grazing incidence the mirror substrates or shells must be very thin and hence low mass, but must also be held in a rigid, stiff structure so that the angular resolution is maintained. The idea of using square pore optics in an approximate form of Wolter Type I geometry was suggested in 1998 [13], but at the time such optics could only be manufactured from glass which provides a very favourable area to mass ratio but was, and still is, unable to meet the high angular resolution requirements of XEUS. The use of Silicon wafers from semiconductor industry [14] offers a solution.

The XEUS sensitivity also depends on the background, which consists of unrejected non-X-ray background arising from the radiation environment in which the observatory operates, of the local Galactic “foreground” emission and of the unresolved extragalactic (AGN-related) component. This background scales with the extraction diameter used to search for photons from a point-like source on the sky. For this analysis an 80% encircled power diameter of 4'' and 10'' \varnothing has been used, depending on the goal (2'' HEW) and requirement (5'' HEW) resolution of the telescope, respectively. For the non-X-ray background we conservatively assume $5 \times 10^{-3} \text{ cts cm}^{-2} \text{ s}^{-1} \text{ keV}^{-1}$ for the WFI, which is the value measured by the XMM pn-CCD camera, and a factor of 10 better for the HXI. The estimate of the local Galactic “foreground” emission is based on the BeppoSAX

Silicon pore optics can provide the lightweight high-resolution X-ray mirrors for XEUS. The pore optics is manufactured using highly polished ($\sim 3 \text{ \AA}$ rms roughness) and flat ($< 0.2 \text{ \mu m}$ over $25 \times 25 \text{ mm}^2$) silicon wafers of 750 \mu m uniform thickness ($< 3 \text{ \mu m}$ PTV) and 30 cm diameter. These wafers are produced as *standard* items by industry and most fortuitously have a surface finish and figure which are tailor-made for X-ray optics. The wafers are cut into rectangular sheets $\sim 10 \times 10 \text{ cm}^2$ and ground and polished on one face to introduce a small taper in thickness ($\sim 1 \text{ \mu m}$ change in thickness from edge to edge). Rectangular channels or grooves (which will become the pores) are cut using a computer controlled diamond saw across one face of each wafer. The uprights between the grooves will form the sidewalls of the pores. These surfaces and the bottom of the grooves are left rough by the sawing process, which neatly suppresses unwanted X-ray reflections. The opposite surface of each wafer, without the grooves, is then coated with high-Z material (Ir, Pt, Au or a multi-layer structure) and possibly overcoated with a thin layer of carbon. Thin strips are masked off during the coating process to leave them bare for bonding to the comb-like structure of the next wafer. The coated surfaces will provide the X-ray mirror reflecting surface within each rectangular pore.

The wafers are then robotically assembled into a stack using a conically profiled mandrel to set the accurate form required for the approximate Wolter I geometry. As each wafer is bent and introduced into the stack it is bonded to the previous wafer by a cold-weld process. This is initially an optical bond because the surfaces (the top of the sidewalls on one wafer and the bare strips between the coating on the opposite wafer) are extremely flat and clean. Additional application of pressure and/or heat produces a partial chemical bonding. Up to 100 wafers are integrated to form a complete high performance pore optic (HPO). Many further details of the processes required to produce the HPOs are given in [15]. The programmatic required for the large-scale production of the silicon pore optics is discussed in [16]. Much of the HPO assembly must be automated to achieve high production speeds and the necessary clean conditions.

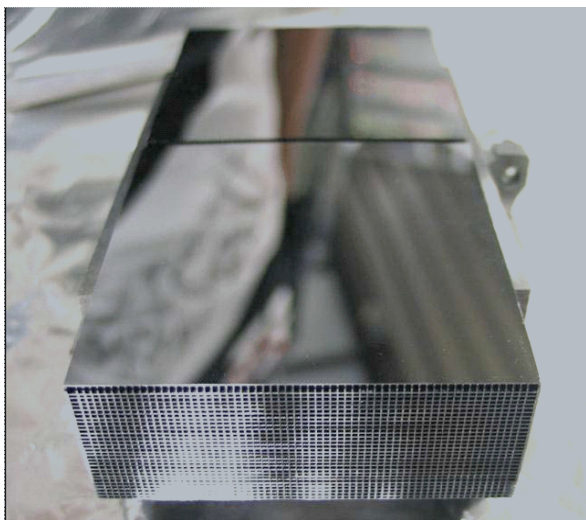


Figure 5.2: Prototype XOU X-ray lens – courtesy Cosine Research

Two HPOs must be assembled and co-aligned in a tandem pair or X-ray Optical Unit (XOU) (Fig. 5.2). X-rays are reflected once from the tangential outer walls of the rectangular pores in the first HPO and once from the corresponding surfaces in the second HPO. The HPOs are aligned to form a conical approximation to the Wolter I grazing incidence geometry. Each XOU therefore acts as an off-axis X-ray lens with aperture dimensions $\sim 10 \times 10 \text{ cm}^2$ and $\sim 20 \text{ cm}$ axial length. Each XOU must be positioned and aligned in modules (petals), which together form an optic with a single X-ray focus. It is remarkable that once the reflecting surfaces within an XOU are correctly aligned, the alignment of individual XOUs in the petal structure is much less critical. The assembly of silicon pore optics into a modular structure is discussed by [17].

The size of the pores, the size of the annular aperture, and the focal length determine the collecting area as a function of energy and the limiting angular resolution that can be achieved. The effective collecting area of each XOU depends on the size of each pore, the thickness of the pore walls, the grazing angles of reflection, the surface coating, and the X-ray energy. A substrate and rib thickness of 150 \mu m and wafer thickness of 750 \mu m enables a pore structure of $0.6 \times 1.5 \text{ mm}$ with $\sim 70\%$ aperture efficiency, which results in a low energy collecting area of $\sim 70 \text{ cm}^2$ for an XOU. An overcoat of carbon on the iridium-coated reflecting surfaces of HPOs can provide enhanced low energy reflectivity [18].

To obtain a low energy collecting area of $\sim 5 \text{ m}^2$, about 1000 XOUs must be assembled into a dense array of X-ray lenses covering an annular aperture. An inner annular radius of 0.67 m , limited by the MSC launch adapter, accommodates HPOs with small grazing angles such that the collecting area at 10 keV is $\sim 0.8 \text{ m}^2$. If multi-layer coatings are used on the inner HPO the high energy response can be extended to give $\sim 0.1 \text{ m}^2$ at 30 keV [18]. An outer aperture radius of 2.1 m can be accommodated within the launcher fairing including a baffle skirt of width $\sim 16 \text{ cm}$.

For such a configuration a minimum focal length of $\sim 35 \text{ m}$ is required to give an effective area of 2 m^2 at 7 keV , and a limiting angular resolution of $< 2 \text{ arcsec}$. Larger focal length increases the effective area at the higher ener-

gies, but also the mass of the optics. The chosen pore size is consistent with a diffraction limited angular resolution < 2 arcsec.

Table 5.2: XEUS X-ray optics requirements

Item	Requirement	Goal
Angular resolution HEW	5 arcsecs	2 arcsecs
Collecting area at 1 keV	5 m ²	5 m ²
Collecting area at 7 keV	2 m ²	2 m ²
Collecting area at 30 keV	400 cm ²	1000 cm ²
Field of view diameter	20(1 keV);15(7 keV);10(30 keV)	

Table 5.4: Optics error budget

Specification (arcsec)	Inherent	Intrinsic	Extrinsic	Environment	Total
Goal	1.4	1.2	0.5	0.5	2.0
Requirement	1.8	3.7	2.0	2.0	5.0

Contributions to the operational angular resolution can be sub-divided into 4 categories: (1) the inherent properties of the conical approximation to the Wolter I geometry and diffraction as discussed in [19, 20], (2) intrinsic manufactured properties of the individual HPOs/XOUs or X-ray lenses, (3) extrinsic elements involving the alignment of the XOUs into the full mirror assembly and (4) environmental effects including thermal distortions, alignment of the mirror and detector spacecraft, stability of the aspect solution etc.. First-cut estimates of the HEW contributions in arcsec are given in Tab. 5.4. The major factors which must be included in the angular resolution budget are intrinsic (e.g. conical approximation, figure errors, micro-roughness and alignment errors, in particular for the two HPOs), extrinsic (e.g. the alignment of XOUs into the aperture array), and environmental (e.g. thermal loading, spacecraft positioning errors and boresighting). The inherent and intrinsic terms associated with the design and manufacturing of the XOUs are dominant. In order to reach the goal of 2 arcsec it may be necessary to reduce the effect of the conical approximation using smaller pores and thereby reducing the length of the reflecting surfaces: this is part of the optimization task. This budget is preliminary and we expect the distribution of the angular resolution budget to be revised through further analysis and experimental verification.

Fig. 5.3 shows the synthesized PSF for the first prototype XOU as derived from pencil beam measurements. A local effective HEW of 3.8 arcsec in this first try is very encouraging when compared with the requirement of 3.7 arcsec. The result displayed is not definitive because the prototype does not include high-Z coating or tapering to give a conical approximation to a Wolter Type I geometry and there are aspects of the geometry which are not

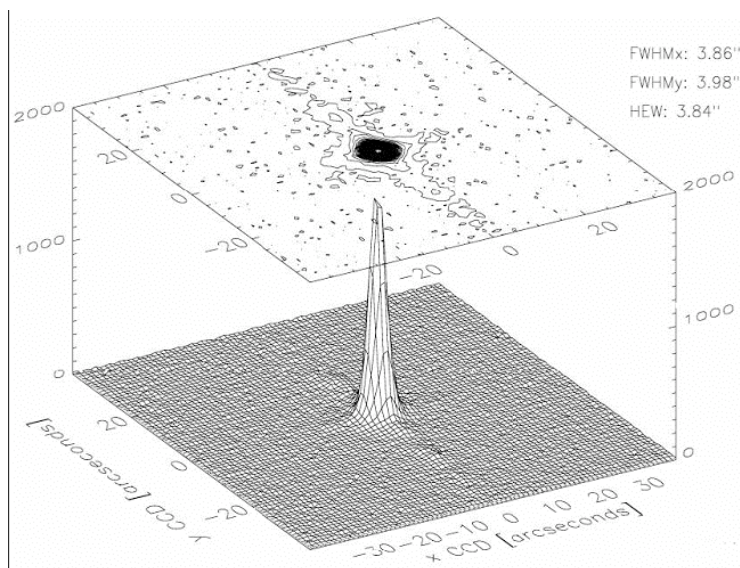


Figure. 5.3: The PSF of the first prototype XOU derived by pencil beam testing at BESSY. The effective HEW is 3.84 arcsec but after allowing for the figure errors known to exist in the mandrel used for the HPO stacking the effective HEW is 2.6 arcsec.

Table 5.3: Optics Characteristics

Characteristic	Value
Pore size	0.6 x 1.5 mm ²
Aperture radii	0.67–2.1 m
Grazing reflection angles	0.27–0.86 degrees
Focal length	35 m
Plate scale	170µm/arcsec

Table 5.5: Optics mass budget

Si	support	ancillary	Total
882 kg	176 kg	238 kg	1296 kg

probed by this test. However, the signs are very encouraging and indicative that the intrinsic error allocation can be met. Further development and testing is required to fully characterise the limiting resolution performance of the XOUs.

The total mirror mass is dominated by the Si plates and is critically dependent on the size of the pores and the thickness of the walls. We have estimated the mass required to meet the effective area requirements at 1 keV and 7 keV using the current parameters for the Si pore manufacture and assuming an aperture annulus of 0.67m<R<2.10m with an effective dead area based on existing petal blocking fractions. We will require ~30,000 Si wafers cut into ~200,000 Si plates and integrated into ~1000 XOUs. In addition we include the structure mass required to support the Si and mass required for an-

cillary items like X-ray/optical baffles, a Sun-shield, thermal control items integrated into the mirror assembly and possibly a background particle rejection system.

The predicted on-axis collecting area as a function of energy, using an iridium reflection surface with a carbon over-coat on the Si units used to derive the mass estimates, is shown in Fig. 5.4. The decline of the XEUS mirror area with off-axis angle is displayed in Fig. 5.5 for two different photon energies.

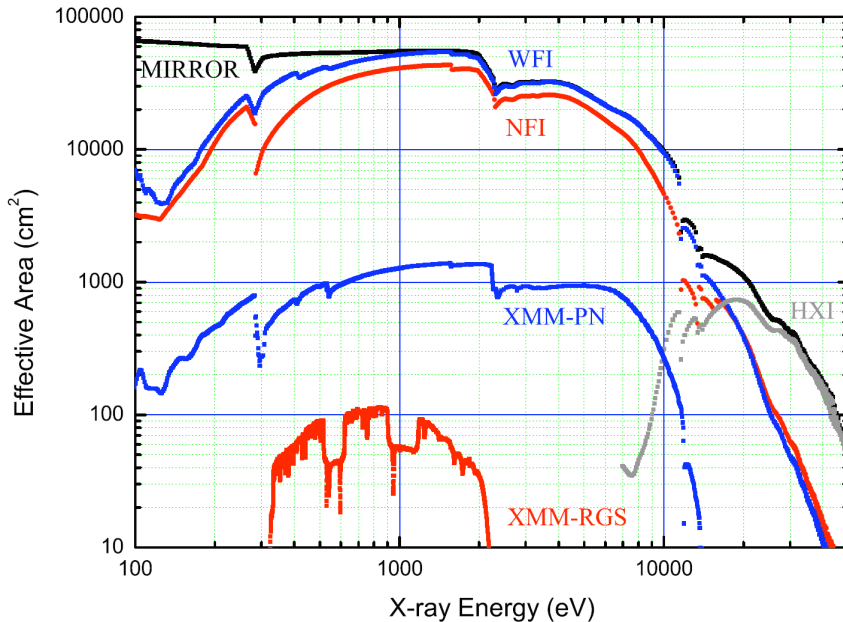


Fig. 5.4: Effective area of the X-ray optics alone and the X-ray optics in combination with the various instruments. The area of the WFI and HTRS are actually equal and are $>5 \text{ m}^2$ between 1–2 keV. The area of the NFI peaks at about 4 m^2 between 1–2 keV. All instruments have lower collecting area below 1 keV, because of the necessary entrance windows and filters. At energies up to about 15 keV the WFI, NFI, and HTRS closely follow the area provided by the optics. Above about 15 keV the HXI takes over. The areas for the XMM-pn and for both XMM-RGSs are shown for comparison. Note the factor 30–40 between XMM-PN and XEUS-WFI, and the factor 400 between the XMM-RGSs and the XEUS-NFI.

The decline of the XEUS mirror area with off-axis angle is displayed in Fig. 5.5 for two different photon energies. The area to mass ratio at 1 keV provided by the Si pore design is $\sim 38 \text{ cm}^2/\text{kg}$ which is the critical advantage for this technology. The carbon over-coat fills in the dips due to the Iridium absorption edges at $\sim 2 \text{ keV}$ and enhances the low energy effective area. If the reflecting surfaces of the XOUs near the inner edge of the aperture are coated with the appropriate multilayers, Pt/C for example, the energy response can be extended to $\sim 30 \text{ keV}$ as indicated. Optimization of the multilayer design and using a smaller inner radius for the aperture (fixed at 0.67 m in the present design) may help to achieve the goal of $\sim 1000 \text{ cm}^2$ at 30 keV.

In our baseline scenario we recognise that the procurement of the mirror is an industrial activity which could well be undertaken under national

funding by a PI team, funded by member states. We have indications that several member states would be willing to take up this responsibility. Until the selection of instrument PIs (2010) we expect ESA to continue the technology developments for the XEUS optics.

There are still major technological issues in the mirror programme which require further research and development. These include:

- Integration of Si plates which have been coated with Ir or similar X-ray reflecting surface into an HPO stack
- Slope errors of the reflectors due to dust particles etc. and control of the conical approximation using mandrels and wedged substrates
- Assembly and verification of a fully representative XOUs with the Wolter I geometry
- Thermal and vibration robustness of an XOUs – robustness of the Si-to-Si bonding in the stacks and their long term stability
- Integration of an array of XOUs to produce a petal with a common focus
- Investigating the need and implementation of an active alignment system at petal (or some other) level
- Thermal environment/control of the mirror assembly. The optics has to maintain its 2–5 arcsec resolution cooling down to about -100 C in the MSC.
- X-ray/optical baffle design for the mirror assembly – there is a strong stray light component because there is no tele-

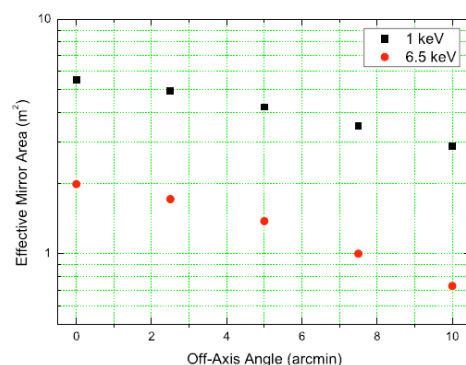


Figure 5.5: Effective area of XEUS optics as a function of off-axis angle for 1 and 6.5 keV

- scope tube between the MSC and DSC – detailed X-ray and optical ray tracing analysis required
- Particle flux suppression/rejection by a magnetic deflector on the mirror assembly

The Wide Field Imager (WFI)

As the main focal plane imaging detector, the purpose of the WFI is to provide 7x7 arcmin² images in the 0.1–20 keV energy band with spectral and time resolved photon counting. Since the plate scale for 35 m focal length equals 170 micron/arcsec, the chosen pixel size of 75 micron is enough to oversample images of 2 arcsec HEW

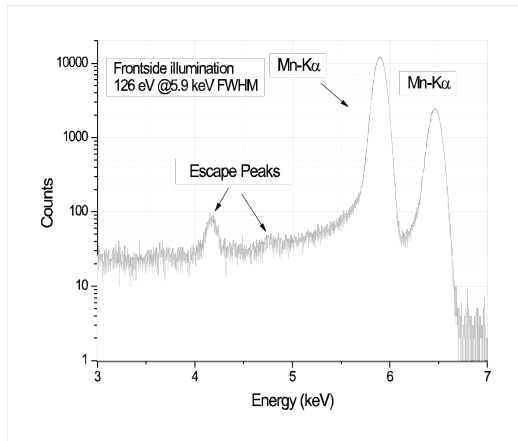


Figure 5.6: Energy response at 5.9 and 6.4 keV from ⁵⁵Fe X-rays

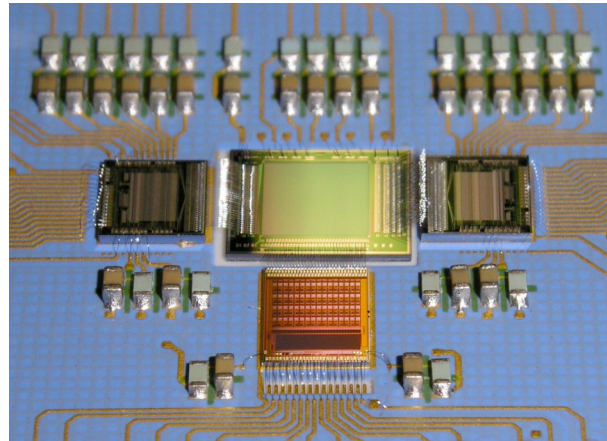


Figure 5.7: Breadboard showing a DEPFET array with clocking and read-out electronics

resolution. Design drivers for the wide field imager are the large number of pixels combining a wide FoV with high spatial resolution, in combination with high read-out speed, good energy resolution and high quantum efficiency over a large energy range. Homogeneous response to radiation and unprecedented long term stability are also essential. This required the development of new Active Pixel Sensor (APS) technology, allowing for the read-out of partial and full images simultaneously. The WFI proposed is an active pixel sensor based on the **D**epleted **p**-channel **F**ield **E**ffect **T**ransistor (DEPFET) concept [21]. As charge transfer in the detector body is not needed due to the local amplification of the signals, **C**harge **T**ransfer **I**nefficiency (CTI) related radiation damage is no longer an issue. The detection sensitivity is determined by the large effective area, the high spatial resolution, and the low background of the instrument. Given the two-spacecraft configuration for XEUS X-rays originating from the sky area outside the telescope FoV could contribute to the instrument background. To restrict this, the instrument requires a 7.9 metre long baffle of 1.0 m diameter in combination with a 16 cm skirt mounted on the MSC. About 107 kg is estimated using a crude design with the baffle being a structural element of the DSC. A detailed baffle design activity, optimizing MSC skirt width versus baffle length could further reduce baffle length and mass or result in a potential increase in the WFI FoV.

The WFI meets the scientific requirements as given in Tab. 3.1. The sensitivity of 3×10^{-18} erg s⁻¹ cm⁻² can be achieved by the current design within a 1 Ms observation time (Fig. 5.1) and 2 arcsec spatial resolution. The effective area is shown in Fig. 5.4.

The DEPFET (see Fig. 5.6 and 5.7), the core of the WFI instrument is being developed by MPE Garching not only for XEUS but also for other X-ray instruments/missions carried out in collaboration with the University of Leicester (BepiColombo) and the University of Tübingen (Simbol-X). The MPI-HLL, jointly operated by MPE and the MPI for physics, is already working on the integral camera design of all three missions. The high speed ASICs are currently developed in cooperation with the electronics groups of Politecnico di Milano/ INFN. International partners with expertise in the field will be invited to join the WFI development.

Critical development areas for the WFI are:

- Increase of the array size from 256 x 256 pixels to the full 1024 x 1024 pixels
- Improvement of the read-out speed of the ASICs from 2×10^6 pixel s⁻¹ to 5×10^6 pixel s⁻¹ (multiplexing 16:1)
- Light blocking filters integrated on the sensor entrance surface

The Hard X-ray Imager (HXI)

The HXI [22] covers a FoV of 7×7 arcmin² with almost 100% efficiency in the 10–40 keV band with $\Delta E < 1$ keV up to 40 keV (Fig. 5.8). To meet this quantum efficiency 0.5 mm thick double-sided CdTe strip detectors are proposed. The 70×70 mm² large FoV detector is built up from 200 micron wide strips to guarantee excellent imaging. To observe the 5–40 keV energy band simultaneously, the HXI is directly mounted below the WFI (Fig. 5.9). In order to obtain high sensitivity (low background), the CdTe detector is actively shielded by a 2 cm thick BGO scintillator. A full background rejection system, composed of active and passive graded shield is also in study at CEA and APC, Paris, taking into account the mission design of Simbol-X, Monte-Carlo simulations, and measurements from the Integral/IBIS mission. At least one layer of a Double-sided Silicon Strip Detector (DSSD) is planned between the CdTe detector and the WFI. This shields the WFI from fluorescence lines emitted by CdTe, and acts as an excellent imaging spectrometer for photons around 10–20 keV.

Both the CdTe and the DSSD are read-out by the same ASICs that requires only 250 μ W/channel.

The collimator (baffle and skirt) for the WFI has to be made opaque to X-rays up to 40 keV. A high-Z tapered metal coating of the WFI baffle with total weight of about 31kg will be required. The HXI meets the scientific requirements for the mission as formulated in Tab. 3.1. The effective area is shown in Fig. 5.4. In the case of the HXI, the European PI of the WFI will receive the HXI from Japan and integrate it with the WFI before delivery to the prime contractor.

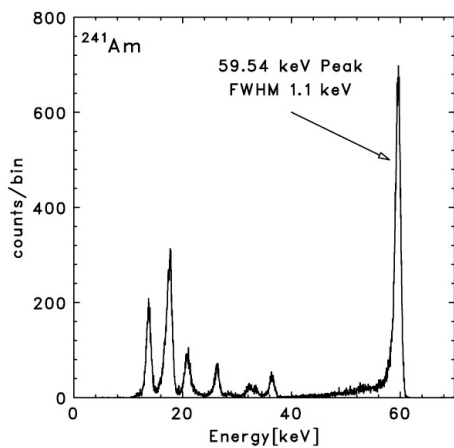


Figure 5.8 : Energy spectrum for CdTe pixel detector read-out with custom design ASIC

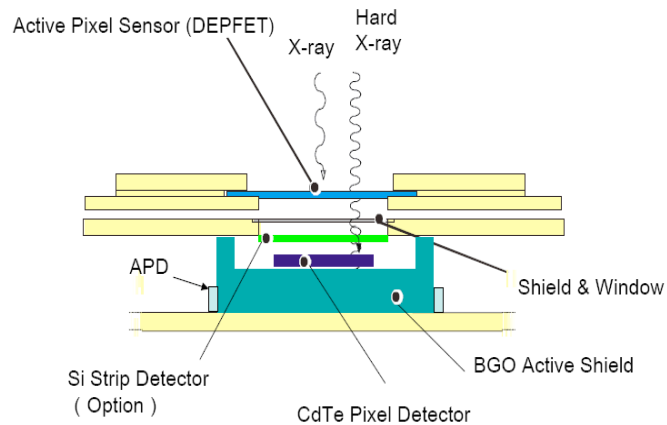


Figure 5.9: Schematic drawing of the Integration of HFI behind WFI

ISAS/JAXA has been developing the HXI, and a breadboard with excellent performance exists. Since the concept of the HXI on XEUS comes from the HXI on the Japanese NeXT mission, which is proposed to be launched in 2012, most of the detector components can be prepared based on the experiences with NeXT. International partners with expertise in the field will be invited to join the HXI developments.

Critical items of this instrument are:

- The CdTe double-sided strip detectors are recently developed at ISAS, based on the long experience with CdTe pixel detectors. The strip detectors still need elaborate in-depth performance testing
- The analogue ASICs used in the laboratory meet the requirements. Testing against radiation tolerance in space environment is required

The Narrow Field Imager (NFI)

This instrument offers imaging spectroscopy with excellent energy resolution and high detection efficiency in the 0.1–20 keV band over a 1.6×1.6 arcmin² FoV. The instrument proposed is based on micro-calorimeter pixel arrays with normal-to-superconducting phase transition thermometers, often called transition-edge-sensors (TES) [23]. Recent experiments at the BESSY synchrotron facility show that the TES technology enables excellent performance over the complete XEUS energy band (Fig. 5.10, 5.11). Therefore the need for a second NFI, based upon superconducting tunnelling junction (STJ) detectors covering the low energy range is removed.

To cover a 1.6×1.6 arcmin² FoV a central imaging array of 32×32 pixels of $240 \mu\text{m}$ size (0.8×0.8 arcmin²) and $100 \mu\text{s}$ fall time is surrounded by 768 pixels of $490 \mu\text{m}$ size and $300 \mu\text{s}$ fall time. An anti-coincidence detector is mounted behind the pixel array. The non-rejected background will be dominated by secondary events produced in the spacecraft, and cryostat. A careful design (material choice, graded shields) in combination with Geant

simulations and follow-on tests should result in a background level similar to Suzaku XRS, i.e. 5×10^{-3} counts $\text{cm}^{-2} \text{s}^{-1} \text{keV}^{-1}$, although the L2 orbit has a 2–3 x higher background than the near earth orbit of Suzaku (~ 0.9 counts $\text{cm}^{-2} \text{s}^{-1}$). The instrument requires cooling to 50 mK for the sensor array with the cold electronics, and anchor harness requiring mounting at 1 K and 4 K, respectively. Instrument heat loads are about $2 \mu\text{W}$ at 50 mK and 1 mW at 4 K. The 1792 pixels will be read-out by about 44 electronics channels making use of frequency-domain-multiplexing (FDM) in the 1–10 MHz band. Base-band feedback will be used to linearize the intrinsically nonlinear SQUID-response. This approach significantly reduces the required harness and consequently the thermal load on the cooling system. To achieve the required sensitivity the improvement in background rejection efficiency (2–3x) above what was achieved on Suzaku will be crucial.

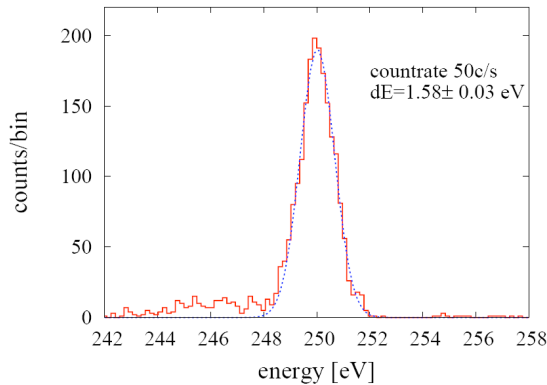


Figure 5.10: Single pixel response to 0.25 keV X-rays with 1.58 eV FWHM energy resolution. Low energy tail is due to X-ray absorption outside the TES-absorber, which will be solved for new array layouts

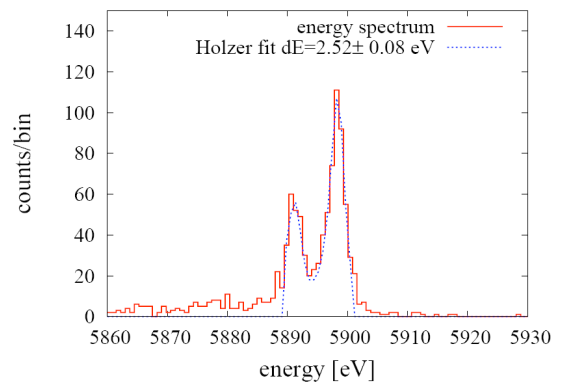


Figure 5.11: Single pixel response to Mn-K $\alpha_{1,2}$ X-rays @ 5.9 keV with 2.52 eV FWHM energy resolution. Low energy tail is due to absorption outside pixel absorber

For the NFI SRON is developing a 5x5 pixel array prototype instrument (EURECA) with several international partners. Presently EURECA contributions come from INA/Zaragoza (LC-filter tuning), ICMA/Zaragoza and IMM/Madrid (MoAu-bilayers), VTT/Helsinki (SQUIDs/FEE), PTB/Berlin (SQUIDs), TMU/ISAS/Tokyo (Electronics), INFN/Genua (TES/electronics), INAF/Rome (calibration), IFCA/Santander and Geneva Observatory/ISDC (Software). The consortium is open to any appropriate international collaboration.

The overall performance demonstration of a 5x5 array read-out with FDM is planned for end 2008 (EURECA Program). Additional effort will be devoted to LC-filters, SQUIDs, FDM with base-band feedback, and cold head design in a TRP and a GSTP contract both starting by autumn 2007.

Critical developments for the NFI are:

- Single pixel optimization, integration of TES with X-ray absorbers; Array manufacturing and qualification (working 5x5 arrays do exist, semi-functional 32x32 arrays have been made)
- Background rejection (anti-coincidence detector, interpixel anti-coincidence, shielding) optimization
- LC-filter and SQUID optimization, together with electrical read-out system
- Cold head design; electrical interconnection techniques; integration in cryostat
- Cooling system

The High Time Resolution Spectrometer (HTRS)

This instrument will provide time resolved single photon spectroscopy for bright point sources up to count rates of 2 Mc s^{-1} . It is based on a Silicon Drift Detector (SDD) [24]. The SDD (Fig. 5.12) is a high speed non-imaging spectrometer enabling count rates of up to $10^5 \text{ c s}^{-1} \text{ pixel}^{-1}$ with good energy resolution close to Fano limited performance for silicon. A 19-pixel SDD is proposed to meet the requirements. The instrument can have a particularly high bit rate of 500 kbits s^{-1} , which on special occasions should be telemetered directly. In normal operation the data will stream in a 19Gbit memory and will be sent to the ground at about 50 kbit s^{-1} . The instrument must be operated out of focus by about 10 cm to distribute the X-ray flux over the full detector array (1.5 cm diameter). CESR is expected to build the HTRS (focusing on the FEE and DPU), with the detector provided by the MPE/MPI-HLL. International

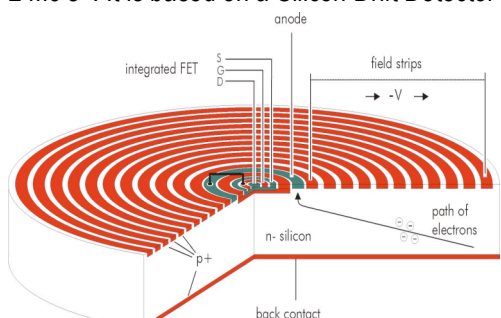


Figure 5.12: Cylindrical field rings to drift electrons to central amplifier

partners with expertise in the field will be invited to join the HTRS consortium.

There are no critical items for this instrument.

The X-ray Polarimeter (XPOL)

The X-ray Polarimeter is based on a gas pixel detector with 50µm pixel size [25,26]. The X-ray photon is absorbed by an atom of the gas and a photoelectron is ejected in a direction which carries the memory of the polarization direction of the photon. The secondary electrons of the ionization track created in the gas by the photoelectron

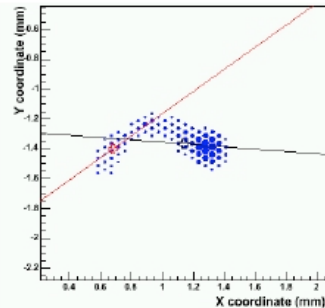


Figure 5.13: Measured event track with interaction point and emission direction reconstruction

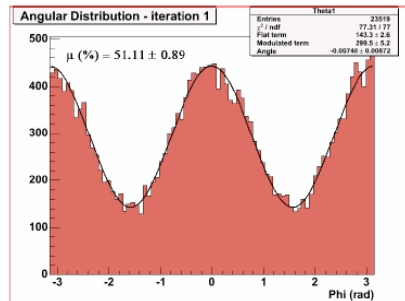


Figure 5.14: Measured modulation curve for nearly 100% polarized photons at 5.4 keV in He-DME (20-80) mixture

are drifted to a Gas Electron Multiplier, which amplifies the charges in a proportional manner. These are then collected by an array of metal pads, the pixels of this imaging device. These pads are the top layer of an ASIC VLSI chip, including a complete read-out chain for each pad, amplifying the charge collected. An algorithm identifies the interaction point and evaluates the emission

direction of the track. The performance of the detector as a polarimeter is based mainly on the quantum-efficiency and on the modulation factor. The selected thickness and composition of the gas-mixture is a trade-off to maximize the sensitivity for a source with a photon spectrum proportional to E⁻².

The measured performance already meets the scientific objectives. More gas mixtures will be simulated and a subset tested to try to extend the energy band to lower energies to increase the sensitivity for soft sources (isolated neutron stars, blazars) and to higher energies, mainly to improve energy resolved polarimetry.

The detector and interface electronics will be built by INFN/Pisa. A potential contractor for the gas cell manufacture is Oxford Instruments, FI, while the Control Electronics can be outsourced to Alcatel Alenia Space; Italy. International partners with expertise in the field will be invited to join the XPOL consortium.

There are no critical items

5.4 Pointing and alignment requirements for focal plane instruments

Different pointing requirements apply to the MSC and DSC. For the MSC the pointing accuracy need only be sufficient to prevent serious vignetting of the optics. The most demanding requirements are set on the boresight, which is defined by the vector from the centre of the detector in operation (only one at a time) to the centre of the X-ray optics. In addition there are requirements on the orientation of the detector spacecraft with regard to the boresight. The sensitive planes of the detectors have to be perpendicular to the boresight within about 1 degree in order to have a uniform focal distance to the optics across the full FoV. The roll around the boresight has to be such that at the edge of the FoV the same pointing accuracies are obtained as at the boresight. Finally the z-position of the DSC has to be controlled such that the appropriate detector is in the focus of the optics.

Table 5.6: Pointing and Alignment

Pointing and Alignment items	WFI	HXI	NFI	HTRS	XPOL
AMA MSC (arcsec)	10	10	10	10	10
APE MSC (arcsec)	60	60	60	60	60
AMA Boresight (arcsecs) [Absolute Measurement Accuracy]	0.5	0.5	0.5	10	2.0
RPE Boresight (arcsecs) [Relative Pointing Error (drift mins)]	≈10	≈10	≈10	≈10	≈10
APE Boresight (arcsecs) [Absolute Pointing Error]	15	15	15	10	10
LTS Boresight (arcsecs) [Long Term Stability (days)]	≈15	≈15	≈15	≈15	≈15
DSC AMA roll (arcmin)	8	8	40	na	40
DSC APE roll (degree)	3	3	15	-	15
DSC Z mm position accuracy	2.5	5.0	2.5	10	2.5

5.5 Operational modes

All instruments have several operational modes, including check-out and calibration modes with electronics stimuli and different science modes for observation of X-ray sources. The telemetry requirements for these modes are given in Tab. 5.1. On-board data-analysis and data compression are performed by the instrument electronics and processors. Special requirements at the satellite level are not foreseen.

5.6 Calibration requirements

Most instruments will make use of electronic stimuli, radioactive sources, and X-ray sources in the sky for calibration. A significant time at the start of the mission will be allocated to these activities, and thereafter at regular intervals. Cross calibration of the various instruments with other X-ray satellites will be performed using cosmic X-ray sources conventionally observed by X-ray missions for this very purpose.

5.7 Special requirements

The cooler requirements are given in Tab. 5.1. Several of the instruments require cooling to 210–260 K. Passive radiative coolers with a Peltier element for temperature control are proposed.

The NFI requires cooling to 50 mK with a effective cooling power between 2–5 μ W. Cryogen-free cooling systems should be used for XEUS given the heritage from Herschel and Planck in Europe, and of Akari, Smiles, and Suzaku in Japan. Given its heritage European industry has come up with two quite different cooling approaches in the XEUS DSC accommodation study. Astrium has proposed a partly redundant system based on 2 Stirlings from EADS (300 \rightarrow 80 K); 2 Stirlings from EADS (80 \rightarrow 18 K); 2 JT from RAL (18 \rightarrow 4 K); dADR from MSSL (4 K \rightarrow 50 mK). Most of the elements of this chain do actually exist and several have flight heritage. The mass and power allocation is 310 kg (incl. cryostat) and 700 W. Alcatel has proposed a more progressive approach using passive radiators and V-grooves to get to about 50 K. From there onwards they propose a fully redundant chain based upon 2 Pulse Tubes from Air Liquide (50 \rightarrow 18 K); 2 He-3 JT from RAL (18 \rightarrow 2.5 K); Sorption-cooler based ADR from CEA (2.5 K \rightarrow 50 mK). The He-3 JT does need development. The mass and power allocations for this system are 260 kg and 470 W.

ISAS/JAXA has longstanding collaboration with Sumitomo for the development and production of cryogen-free coolers for space. A system for XEUS would most likely exist of two 2-stage Stirlings (300 \rightarrow 18K); two 2-stage Stirlings/JT (18 \rightarrow 4 K); 2 He-3 sorption coolers (1.8 \rightarrow 0.4 K); and 1 ADR (0.4 K \rightarrow 50 mK). Most of these components are existing and have flight heritage. Mass and Power allocations are about 300 kg and 450 W.

Taking the above numbers on mass and power as a reference, we consider 300 kg and 600 W as an adequate resource allocation for the cooling system of the NFI (table 5.1).

Recently excellent performance of a TES instrument at the BESSY synchrotron ($\Delta E < 2$ eV @ 1.8 keV) has been demonstrated. For instrument cooling a Pulse Tube in combination with a double stage Adiabatic Demagnetization Refrigerator has been used, indicating successful shielding for EMI/EMC and sufficient isolation from closed cycle cooler microphonics.

5.8 Current heritage and technology readiness

A summary of the technological heritage at the instrument level is given in Tab.5.7.

Table 5.7: TRL of proposed instrumentation

Sub-system	TRL	comments
X-ray Optics		
Mirror-stack	3	Proof of Principle shown for various stacks
X-ray lens (XOU)	3	Proof of principle demonstrated with measured resolution < 3 arcsec.
Petal	3	Mechanical/Thermal structural model available. Full petal procured in 2008
Optics	2-3	Proof of principle demonstrated in several key areas
Wide Field Imager (WFI)		
DEPFET array	5	256 x 256 pixel array demonstrated with good performance Radiation hardness demonstrated to at least 1 Mrad.
Analog ASIC	5	ASICs in place. Increase of speed (2x) required, ongoing development

Filters	5	Prototype fabricated and tested
Cooler	6	Passive radiators demonstrated on XMM-Newton. Peltier coolers on many others.
EMI/EMC	5	Good system performance demonstrated
Hard X-ray Imager (HXI)		
CdTe sensors	4	Performance demonstrated of CdTe pixel-arrays. Double-sided strip arrays meet performance, but require in depth testing
ASICs	4-5	ASICs performance demonstrated in the laboratory. Radiation hardness to be assessed.
Narrow Field Imager (NFI)		
TES-array	4	Performance demonstrated on single pixels, non fully representative but good performing 5 x 5 arrays produced, and processing of 32 x 32 arrays demonstrated.
Electronics	4	AC-bias of TES pixels demonstrated. SQUIDs (PTB, VTT) and LC-filters (SRON) available close to specification. Frequency-domain-multiplexing with theoretical performance demonstrated in the laboratory
Filters	5	Proven on Suzaku. Optimization for low-energy response
Cooling	4 - 5	Several type of cooler elements demonstrated (TRL > 5). System quite complex (TRL = 4)
EMI/EMC	5	Design proven at recent single pixel calibration at BESSY synchrotron in closed cycle PT + ADR
High Time Resolution Spectrometer (HTRS)		
Sensor	7	Flown on Mars Exploration Rovers (NASA)
Electronics	5	Standard analogue and digital electronics
X-ray Polarimeter (XPOL)		
Sensor	5	Design is quite well tested and only minor optimization is needed to improve efficiency
Electronics	5	ASIC used meets the specifications

6 Spacecraft key factors

6.1 Spacecraft configuration

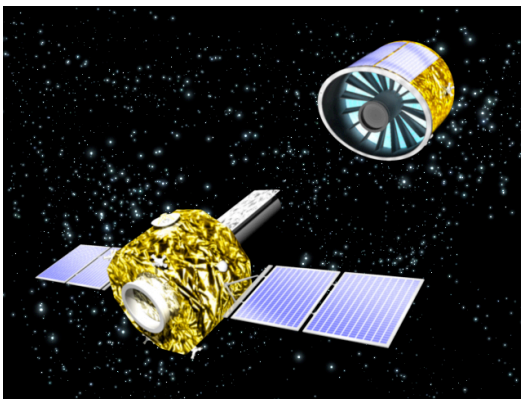


Fig. 6.1: Artist impression of the mirror spacecraft (right) flying in formation with the detector spacecraft

XEUS requires at least a focal length of ~35 m to reach a collecting area of 5 m² at 1 keV and a spatial resolution <5 arcsec (goal 2 arcsec). A longer focal length would reduce the FoV of the instruments. Given the 35 m focal length chosen, a dual spacecraft configuration is essential. The MSC points the optical axis of the mirror at the target, using a classical AOCS with star trackers, etc., and cold gas thrusters (to avoid mirror contamination). The DSC keeps one of the focal plane instruments at the focal point of the mirror. In addition to star trackers which provide the primary attitude reference, its AOCS uses laser and RF rangefinders, with cold gas thrusters, to maintain the formation flying. Both spacecraft (Fig.6.1) are tracked from the ground station; the main downlink for instrument telemetry is in the DSC while the MSC transmits only housekeeping data.

Mirror spacecraft

The MSC is three axis stabilised with the XEUS mirror as the sole payload. The mass of the silicon pore optics mirror is < 1300 kg.

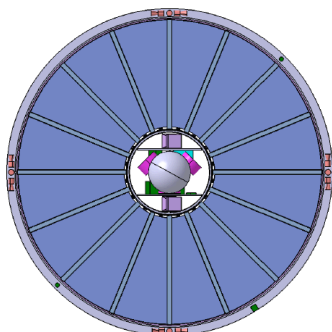


Fig.6.2: On-axis view of the preliminary telescope configuration inside the MSC. The central thrust and

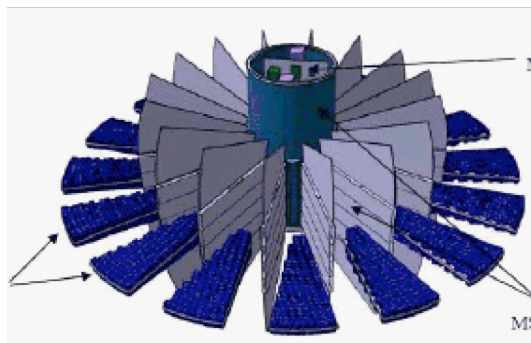


Fig.6.3: Exploded view of the preliminary telescope configuration

the radial vanes support the mirror petals. The mirror petals are surrounded by a cylindrical sun baffle

in the MSC, including support structure, mirror petals, contamination covers and S/C subsystems. The cylindrical sunshield surrounding the above unit is not shown in this picture

The inner 0.67m radius of the optics is dictated by the 120 cm diameter of the Ariane launch adapter. The spacecraft subsystems are contained inside the central thrust cylinder (Fig.6.2; 6.3), which attaches to the launcher adapter. The outer radius of 2.1 m is limited by the diameter of the Ariane fairing. The mirror petals are supported by the radial CRFP structure and the central thrust cylinder. The optics is surrounded by a cylindrical sunshield with solar cells on the sunward half of the sunshield. An annular skirt of 16cm is mounted between the mirror and the cylindrical sunshield (Fig.6.4). This, together with the MSC sunshield and the DSC baffles, blocks X-rays and stray light from the instrument fields of view. The total wet mass of the MSC (including margin) is 4200 kg (see Tab. 6.1 for details).

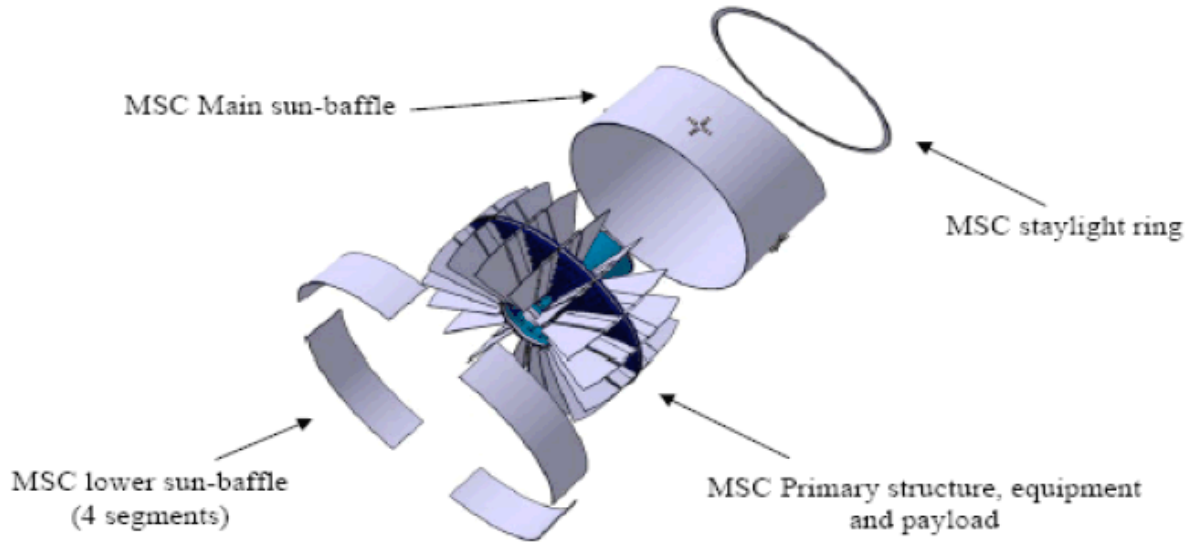


Fig.6.4: Exploded view of the preliminary telescope configuration (MSC), including the cylindrical sun baffle, and the stray-light skirt.

Table 6.1: Mass and power estimates for the MSC including 20% contingency

ITEM	MASS (KG) (INCL. 20%)	POWER (W) (INCL. 20%)	COMMENT
Mirror	1840		Includes baffles and heat pipes for passive thermal control, and 30% development contingency
Spacecraft Structure	900		
Covers and Mechanisms	200	95	Power for deployment of covers only
Thermal Control	120	45	Thermal control of the mirror is mainly passive
AOCS	90	100	
Propulsion	35	68	
Power system	45	-	
Harness	110	9	
Communications	25	99	
Data Handling	10	26	
Total Power		442	
Total Dry Mass	3375		
20% System Margin	675	88	
Propellant	150		
Total Power		530	
Total Wet Mass	4200		

Detector spacecraft

The Detector Spacecraft carries the instrumentation payload and the formation-flying package that keeps the prime focus located on the centre of the relevant instrument FoV. The spacecraft is three-axis stabilised and electrical power is provided by deployable solar panels. It also provides the stray light baffles, the cooling necessary for the focal planes, and the main data downlink. Fig.6.5 shows a 3D-drawing from one of the industrial accommodation studies of the DSC. Clearly visible is the central baffle of the WFI/HXI that also serves as a structural element for the spacecraft. The main challenges for the DSC are the formation flying package and the cooling system for the NFI. The wet mass of the DSC (including margin) is 2125 tonnes (see Tab. 6.2). The total mass that can be launched by the Ariane 56 ECA is 6400 kg, which matches the predicted total spacecraft wet mass of 6325 kg.

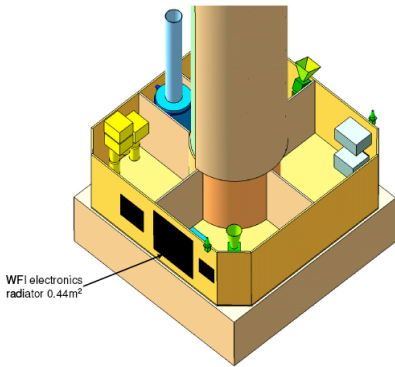


Fig.6.5: Accommodation of the WFI/HXI with the central 8 m long baffle. The blue instrument behind the central baffle is the NFI. The lower unit contains the S/C subsystems

Table 6.2: Mass and power estimates for the DSC

ITEM	MASS (kg)	Equipment margin 20%	Comment	Power (W)	Equipment margin 20%	Comment
Total WFI	187	37	Baffle is CFRP	260	52	
Total NFI	358	72		812	162	
Total HXI	70	14	Baffle + Au 240µ tapered	46	9	
Total HTRS	23	5		71	14	
Total XP	23	5		34	7	
Total Payload	661	133	Incl. all coolers	1223	244	
PLM Bus	233	47		51	10	
Total P/L Module	894	180	Total P/L Module	1274	254	
Service Module	457	91		450	90	Estimate
Inter S/C adapter	25	5	Total Power	1724	344	
Total Mass	1376	276	Total S/C power	2068		
Total S/C Mass	1652		20% sys. Margin	414		
20% sys. margin	330		All Up Power	2482		
Propellant	143					
All Up Mass	2125					

6.2 AOCS requirements

The instrument requirements are given in section 5.3. From those requirements it is clear that the MSC requires standard 3-axis stabilization with modest accuracy. The DSC however requires in addition a formation-flying package to keep the boresight between instruments and mirror within the necessary constraints.

Sky accessibility is dominated by the need to control the temperature gradients in the mirror and the avoidance of stray light. The bore sight of the two spacecraft system will be generally at right angles to the solar vector, with a range of beta angles $\pm 5^\circ$ ($\pm 15^\circ$ goal). This will provided access to any celestial object over 6 months, and allow continuous observations for a minimum of 10 days (30 days goal)

6.3 On-board data handling and telemetry requirements

Tab. 5.1 identifies the maximum and typical telemetry rates for each instrument are given. The baseline for the instruments is that data processing and packaging is taken care of within the instruments electronics. The on-board data handling electronics should be regarded as an interface between the spacecraft telemetry and the instruments, thereby allowing for commanding as well as data acquisition from the instruments. Obviously the system has to be designed within the constraint set by operations at L2.

6.4 Mission operations concept (ground segment)

Mission operations are in two phases: the cruise to L2 plus the establishment of formation flying, followed by the scientific observation phase. The cruise and formation flying will be controlled by the MOC provided by ESA, with support by the Prime. Subsequent scientific operations will be controlled by the XEUS SOC. For this proposal we assume 5 years of scientific operations as described in section 7.

6.5 Estimated overall resources (mass and power)

See Tab. 6.1 and 6.2 for detailed mass and power estimates of the MSC and DSC.

6.6 Specific environmental constraints (EMC, temperature, cleanliness)

The Mirror is very sensitive to contamination, both particulate and molecular. The general requirements used for XMM-Newton should be observed. In addition, because the mirror will operate at low temperature, particular attention should be given to condensables from the spacecraft and the thruster plumes. The mirror temperature should be as high as can be achieved with a largely passive system using heat-pipes and radiators; a lower temperature limit should be set which will prevent water condensation at the prevailing partial pressure: e.g. -60 °C for a partial pressure of 10^{-12} Pa.

6.7 Current heritage and technology readiness level

Table 6.3: Current heritage and technological readiness

Sub System	TRL	Comment
10K Stirling cycle cooler	6-7	Based on 50–80K Stirling cooler of which 13 are successfully flying
50–80K Stirling cycle cooler	6-7	As above (standard product). baselined for instruments on MTG and GMES Sentinel 3.
4K J-T cooler	8	Fully qualified for the HFI on Planck
2.5K J-T cooler	6-7	Based on the 4K cooler
300mK Helium sorption cooler	6-7	A modified version of the 300mK cooler fully qualified for Herschel.
50mK ADR	3-4	New development-has undergone pre-qualification vibration test.
R/F metrology for FF	7-8	
Coarse lateral metrology for FF	4	
Fine metrology for FF	4	
Other S/C systems	8-9	"off the shelf"

The DSC design draws on Herschel, Planck and other ESA spacecraft with cryogenic payloads. The main development items will be the baffles, the cryogenic cooling chain, and the formation flying subsystem. The MSC will use standard spacecraft subsystems, with the structure, mirror mounting and baffles being the main development items.

6.8 Proposed procurement approach & international partners

XEUS is a major space observatory and as such requires international collaboration to achieve its aims. The estimated CaC is derived below in section 9, and then two example scenarios on international collaboration are described in detail; these scenarios are backed up by letters of support from the relevant agencies. In each scenario the relevant system-level and payload-level costs for ESA, external agencies and ESA member states are given. Other scenarios are possible including one involving collaboration with China, but these are not detailed here. A scenario based on collaboration with NASA could also be envisaged, but is not included because of the ongoing review of NASA's Beyond Einstein programme.

6.9 Critical issues

Most of the components on board of MSC and DSC are actually quite standard and do not need serious developments. However, as noted earlier, there are several critical issues that need study and further development well in advance of the mission, i.e.:

- thermal control, cleanliness, and baffling of the X-ray optics on the MSC
- formation flying of MSC and DSC.
- fully dry cryogenic system for the NFI

7 Science operations and archiving

XEUS is an observatory mission and as such needs significant investment in its scientific operations and interface with the world community. For XEUS the CaC includes 2 years of scientific operations, after establishment at L2 and the commissioning phase. The scientific operations for this period will be undertaken by ESAC in collaboration with a Swiss PI-led Science Data Centre, following the successful model and division of responsibilities established for INTEGRAL. Switzerland has expressed a strong interest in taking the lead in this consortium.

Mission extensions beyond this period could be done on the same basis. However, in the light of the recent SPRT recommendations to limit the total mission operations cost, a viable alternative is for the complete XEUS SOC activity for mission extensions to be taken over by a European PI consortium, led by Switzerland. The experience gained during the initial two-year period of cooperation with ESAC will allow a smooth transition of full science operations to the PI team. We have used this model to cost five years science operations for XEUS, i.e. three additional years potentially covered by national funds.

The XEUS science operation centre (SOC) will be responsible for the following tasks: guest-observer announcements of opportunity, observation planning, pre-processing of raw satellite telemetry, monitoring instrument performance and observation quality, high-level data product generation, distribution of guest-observer data, data safekeeping and making low-level and high-level data available to the community. In addition, the SOC will be responsible for the development of the analysis software and calibration data, in close collaboration with the instrument teams, as well as for the distribution of this software. The centre will generate all the documentation and support needed to understand and analyze XEUS data. The SOC will also be proactive in the communication of XEUS highlight results to the public. The SOC will create and operate the XEUS data archive.

8 Key technology areas

The key technological elements of XEUS are the X-ray mirror and the formation flying. The lightweight silicon HPO X-ray optic enables the key scientific requirement on XEUS, the 5 m² mirror; formation flying delivers the necessary 35 metre focal length. In addition thermal control of the mirror, and the cryogenic coolers for the payload, are essential to mission success. Formation flying can profit very significantly from ESA studies in the context of Darwin, and ongoing studies of special thrusters and laser metrology systems.

8.1 Current development status

X-ray optics

The HPO silicon pore optics has been developed by ESA to the point where a proof of concept has been demonstrated. The silicon mirror surfaces have been shown to be of adequate smoothness, and suitable heavy metal coatings have been applied; etching the pores and stacking and bonding of the plates has been demonstrated, together with assembly of tandems, which are the stacked paraboloid and hyperboloid elements of the Wolter optic. To demonstrate the complete optical capability requires the plates to be wedged before stacking. Wedging and bonding of the plates has been demonstrated, but a full optic of adequate quality to demonstrate proper focusing has yet to be assembled. We are confident however that this is very close to being achieved. While environmental test are some way off, the stacks are already shown to be robust and capable of retaining their integrity.

Formation flying

The XEUS requirements on formation flying are relatively modest (see Tab.5.6), nevertheless this remains a key technology development. There are a number of ESA studies on-going which have direct relevance to XEUS, including a possible technology demonstrator Proba 3. In addition CNES is planning a formation flying mission with very similar requirements to XEUS (Simbol-X).

Thermal control of the MSC

Keeping such a large mirror isothermal is a challenging requirement and can only be done by allowing it to reach a rather low temperature using passive control: radiators, MLI, heat pipes and baffles. Thermal models indicate that this is feasible. Contamination at these low temperatures has to be addressed vigorously.

Cryogenic coolers

These have been the subject of two DSC industrial studies funded by ESA. Both have produced feasible systems to meet the requirements and the mass and other resources are included in the spacecraft budgets presented in Tab. 6.2.

8.2 Essential future developments

The optics is the most important enabling technology to be further developed. Following proof of concept, the industrialisation of the assembly process, alignment, metrology, and demonstration of a fully representative mirror petal is required. Formation flying, thermal control of the MSC, and cryogenic coolers are also essential development tasks for the future.

9 Communications and outreach

XEUS will be the most challenging X-ray astronomy mission ever accomplished, both from a scientific and a technological point of view. In order to communicate the potential and excitement of the mission and its eventual scientific achievements a detailed communications and outreach plan will be needed, entailing a serious investment of resources. High energy astrophysics is undoubtedly an area that can inspire both young audiences and the public at large. Here we touch on just a few ideas. Targeting XEUS as a unique achievement in *global* collaboration will be the main aim of a more detailed communication and education plan, to be formulated later.

One can distinguish several target groups, each of them requiring a group-specific approach: *Policy makers, Media / press, Broad public, Youth / Students.*

- Weblog / press releases. The full development and operations period of XEUS in terms of progress and highlights, will be portrayed via a weblog, the feeding ground for periodical press releases. This public website about the XEUS mission, stipulating its science goals and the technology will include background material, a hot news section, updates to the progress of the mission e.g. construction of the satellite, observations of the day. Certain sections will be specifically tailored to key target groups, e.g. school children, youth groups, school teachers, parents. This material can be taken up by the ESA science communications office for distribution as ESA press releases.
- Graphics and animations. We will build and maintain a publicly accessible database with high resolution pictures of the mission, free for use. Animations and artist impressions will be produced of the development of the satellite, the principle of formation flying and give details of potential targets of observation.
- Exhibitions. In collaboration with science centers we will develop contributions to exhibitions, highlighting the physics of the violent universe.
- Lectures for the public. Scientists involved in the XEUS project will be available to give popular lectures for broad audience.

10 References

[1] Li Y. et al., 2006, astro-ph/0608190; [2] Gilli R., Comastri A. & Hasinger G., 2007, A&A 463, 79; [3] Fabian, A.C. et al., 2006, MNRAS 366, 417; [4] Hasinger G., Miyaji T. & Schmidt M., 2005, A&A 441, 417; [5] Nicastro, F., et al., 2005, Nature 433, 495; [6] Rasmussen, A.P., 2007, ApJ 656, 129; [7] Fabian A.C. et al., 2002, MNRAS 335, L1; [8] Streblyanska A. et al 2005, A&A 432, 395; [9] Iwasawa K., Miniutti G. & Fabian A.C., 2004, MNRAS 355, 1073; [10] Armitage P.J. & Reynolds, C.S., 2003, MNRAS 341, 1941; [11] Hussain, G.A.J., et al, 2007, MNRAS 377, 1488; [12] Parmar A.N. et al., 1999, A&A 345, 611; [13] Willingale R. et al., 1998, Experimental Astronomy, 8, 281-296; [14] Beijersbergen M. et al., 2004, Proc SPIE Vol. 5488, 868-874; [15] Günther R. et al., 2006, Proc SPIE Vol. 6266-46; [16] Kraft S. et al., 2006, Proc SPIE Vol. 6266-130; [17] Graue R. et al., 2006, Proc SPIE Vol. 6266; [18] Pareschi G. et al., 2004, Proc SPIE Vol. 5488, 481; [19] Willingale R., Kunieda H., Okajima T. and Naitoh M., 2005, SPIE 5900, 124; [20] Mieremet A.L. & Beijersbergen M.W., 2005, Appl.Opt. 44, 7098; [21] Treis J. et al., 2006, NIMA 568, 1, 191; [22] S. Watanabe et al., 2007, NIMA 567, 150; [23] de Korte P. et al., 2006, Proc SPIE 6266, 62661Z; [24] Barret D. et al, 2004, Proc SPIE 5501, 23; [25] Bellazzini R. et al., 2006, NIM A 566,552; [26] Bellazzini R. et al.,2007, NIMA, in press. (astro-ph/0611512)

11 XEUS supporters

Principle Investigators, Co-Investigators, Contributors, Supporters

Ivan Agudo; **David Alexander**; Ali Alpar; Diego Altamirano; **Giovanni Amelino-Camelia**; **Monique Arnaud**; Bernd Aschenbach; **Marc Audard**; Hisamitsu Awaki; Luca Baldini; Jean Ballet; Solen Balman; Aya Bamba; **Xavier Barcons**; **Didier Barret**; Martin Barstow; **Mark Bautz**; Mathias Beck; **Werner Becker**; Volker Beckmann; Ronaldo Bellazzini; Tomaso Belloni; Sudip Bhattacharyya; Stefano Bianchi; Pavel Binko; **Alain Blanchard**; **Johan Bleeker**; **Alex Blustin**; Fabrizio Bocchino; **Hans Böhringer**; Laurence Boirin; **Thomas Boller**; Dominik Bomans; Angela Bongiorno; Hale Bradt; **William Nielsen Brandt**; Graziella Branduardi-Raymont; Johan Bregeon; Alessandro Brez; **Catherine Brocksopp**; Marcella Brusa; Carl Budtz-Joergensen; Luciano Burderi; Maria Dolores Caballero-Garcia; Paul Callanan; **Massimo Cappi**; Patrizia Caraveo; **Francisco J. Carrera**; Jorge Casares; Alberto Javier Castro-Tirado; Sylvain Chaty; Maria Chernyakova; Finn Christensen; Francesca Civano; **Andrea Comastri**; **Enrico Costa**; **Thierry Courvoisier**; **Stanley Cowley**; **Judith Croston**; Jamie Crummy; Antonino D'Ai; Flavio D'Amico; **Michael De Becker**; **Piet de Korte**; Ignacio de la Calle Perez; Domitilla de Martino; **Anne Decourchelle**; Roberto Della Ceca; Jan-Willem den Herder; Ralf-Jürgen Dettmar; Tiziana Di Salvo; **Maria Diaz Trigo**; Vladimir Dogiel; Chris Done; Tadayasu Dotani; **Lionel Duband**; Florence Durret; **Tom Dwelly**; Stefano Etori; Yuichiro Ezoe; **Andrew Fabian**; Lourdes Fabrega; Maurizio Falanga; Rene Fassbender; Philippe Ferrando; Chiara Ferrari; **Alexis Finoguenov**; Fabrizio Fiore; Ettore Flaccomio; **Kathy Flanagan**; Luigi Foschini; **Michael Freyberg**; **Peter Friedrich**; Ryuichi Fujimoto; Yutaka Fujita; **Akihiro Furuzawa**; Roberto Fusco-Femiano; Duncan Fyfe; Luigi Gallo; Poshak Gandhi; Ioannis Georgantopoulos; **Roberto Gilli**; Isabella Maria Gioia; Gabriele Giovannini; Paolo Goldoni; Andrea Goldwurm; Vito Graffagnino; Paola Grandi; **Richard Griffiths**; Nicolas Grosso; Adriano Guarnieri; Manuel Guedel; Martin A. Guerrero; **Yoshito Haba**; **Thomas Hackman**; Pasi Hakala; Valeri Hambaryan; **Günther Hasinger**; Coel Hellier; J. Patrick Henry; Willem Hermsen; Werner Hofmann; Andrew Holland; Allan Hornstrup; Rene Hudec; **Juhani Huovelin**; Rosario Iaria; Manabu Ishida; Yoshitaka Ishisaki; Naoki Isobe; Philippe Jetzer; Roderick Johnstone; Peter Jonker; Philip Kaaret; **Jelle Kaastra**; **Steve Kahn**; Emrah Kalemci; Wolfgang Kapferer; Vladimir Karas; Jun Kataoka; Wolfgang Kausch; Madoka Kawaharada; Noboyuki Kawaii; **Richard Kelley**; Eckhard Kendziorra; Jürgen Kerp; Shunji Kitamoto; Wlodek Kluzniak; Takayoshi Kohmura; Motohide Kokubun; Stefanie Komossa; Katsuji Koyama; Thomas Kronberger; Aya Kubota; **Hideyo Kunieda**; Nicola La Palombara; **Dong Lai**; **Georg Lamer**; Jean Pierre Lasota; Luca Latronico; **Philippe Laurent**; Nora Loiseau; Javier Lopez-Santiago; **Thomas Maccarone**; **Yoshitomo Maeda**; Antonio Maggio; Vincenzo Mainieri; Magdalena Mair; **Kazuo Makishima**; Pino Malaguti; Julien Malzac; Karl Mannheim; Laura Maraschi; Sera Markoff; J. Miguel Mas-Hesse; Marco Massai; Silvia Mateos; Hironori Matsumoto; **Giorgio Matt**; **Mariano Mendez**; Andrea Merloni; Cole Miller; Giovanni Miniutti; Massimo Minuti; **Kazuhisa Mitsuda**; David Montes; Koji Mori; Christian Motch; **Fabio Muleri**; Yujin Nakagawa; Kazuhiro Nakazawa; **Kirpal Nandra**; Yael Naze; Ignacio Negueruela; Jukka Nevalainen; Andrew Norton; Paul O'Brien; Yasushi Ogasaka; **Takaya Ohashi**; Nicola Omodei; Julian Osborne; Lidia Oskinova; Naomi Ota; Hector Oti; Masanobu Ozaki; Frits Paerels; **Mathew Page**; Aina Palau; Stephane Paltani; **Giorgio Palumbo**; Iossif Papadakis; Giovanni Pareschi; **Mikhail Pavlinsky**; Melissa Pesce-Rollins; Pierre-Olivier Petrucci; Elena Pian; Marguerite Pierre; Michele Pinchera; Santina Piraino; Luigi Piro; Manolis Plionis; Etienne Pointecouteau; **Trevor Ponman**; Gabriele Ponti; **Delphine Porquet**; Juri Poutanen; **Gabriel Pratt**; Peter Predehl; Nicolas Produit; John Pye; **Gregor Rauw**; Massimiliano Razzano; **Thomas Reiprich**; **Tim Roberts**; Jerome Rodriguez; **Kathy Romer**; **Gustavo EstebaRomero**; Michael Rowan-Robinson; Helen Russell; Jeremy Sanders; Andrea Santangelo; Jorge Sanz Forcada; Jean-Luc Sauvageot; Richard Saxton; Sabine Schindler; **Robert Schmidt**; Jürgen Schmitt; Axel Schwöpe; **Salvatore Sciortino**; Giancarlo Setti; Carmelo Sgro'; Tariq Shahbaz; K.P. Singh; **Alan Smith**; **Paolo Soffitta**; Simona Soldi; Paolo Soleri; Gloria Spandre; Luigi Stella; Gordon Stewart; **Lothar Strüder**; Michel Tagger; Gianpiero Tagliaferri; **Tadayuki Takahashi**; **Takayuki Tamura**; **Yasuo Tanaka**; Makoto Tashiro; Yukikatsu Terada; Yuichi Terashima; Masahiro Teshima; Jose M. Torrejon; Diego F. Torres; Ginevra Trinchieri; Joachim Trümper; **Yohko Tsuboi**; Hiroshi Tsunemi; Takeshi Tsuru; **Marc Tuerler**; **Martin Turner**; **Yoshi Ueda**; Yuji Urata; Edward van den Heuvel; Michiel van der Klis; Almudena Velasco; **Cristian Vignali**; **Jacco Vink**; Roland Walter; Martin Ward; **Robert Warwick**; **Mike Watson**; **Anna Watts**; Natalie Webb; Julia Weratschnig; Peter Wheatley; Simon White; Ralph Wijers; **Richard Willingale**; Jörn Wilms; Anna Wolter; Diana Worrall; Kinwah Wu; J. S. Yadav; Kazutaka Yamaoka; Noriko Yamasaki; Daisuke Yonetoku; Atsumasa Yoshida; Andrew Young; Silvia Zane; Andrzej Zdziarski; **Nan Shuang Zhang**; Houri Ziaeeepour

12 Letters of support



25 June 2007

Prof. Jean-Jacques Dordain
Director General
European Space Agency
8-10 rue Mario Nikis
F-75738 Paris Cedex 15
France

Dear Prof. Dordain,

Letter of support

I am glad to inform you that eight proposals in the attached list have been prepared under the collaboration between European and Japanese groups and are to be submitted to ESA in response to "Cosmic Vision 2015-2025 Call for Proposals" issued on 05 Mar 2007.

Let me briefly describe the Cosmic-Vision-related activities in Japan. We have standing steering committees for space science and space engineering at ISAS/JAXA to select and promote new science missions. Dedicated working groups have been organized under the steering committees for the future projects being discussed between Europe and Japan under the frame work of the Cosmic Vision. The committees reviewed the projects proposed by the Japanese working groups and reported that the eight projects in the attached list had very high scientific values and clear identification of Japanese roles.

ESA and JAXA have a long history of very successful collaboration on scientific missions, including recently launched Suzaku, Akari, and Hinode. They are now working together on the very challenging mission, BepiColombo, which is scheduled to be launched in 2013. The collaboration scheme between Europe and Japan has been proved to be very effective, and is now expected to be the very best way to pursue more challenging missions in the future.

I fully support the present proposals prepared under the collaboration between Europe and Japan and look forward to working with ESA for the future of space science.

Yours sincerely,

A handwritten signature in black ink, appearing to read 'K. Tachikawa', is written over a horizontal line.

Keiji Tachikawa
President

Encl. List of Cosmic Vision proposals being prepared under the collaboration between Europe and Japan

CC: Dr David Southwood, Director of Science, ESA
Dr Sergio Volonte, Science Head of Planning and Coordination Office, ESA
Mr Chiyoshi Kawamoto, Director, JAXA Paris Office

Japan Aerospace Exploration Agency
Marunouchi Kitaguchi Building, 1-6-5, Marunouchi, Chiyoda-ku, Tokyo 100-8260 Japan
Tel:81 3 6266 6001 Fax 3 6266 6901



List of Cosmic Vision proposals
prepared under the collaboration between
Europe and Japan

This is a list of Cosmic Vision proposals being prepared under the collaboration between Europe and Japan. Dedicated working groups corresponding these proposals are organized under the standing steering committees for space science and space engineering at ISAS/JAXA.

Cross-Scale		
	European P.I.:	Steve J. Schwartz (Imperial College, UK)
	Japanese P.I.:	Kiyoshi Maezawa (JAXA, Japan)
Darwin		
	European P.I. :	Alain Léger (IAS, Univ. Paris-Sud, France)
	Japanese P.I.:	Hiroshi Shibai (Nagoya University, Japan)
EDGE		
	European P.I.:	Luigi Piro (IASF-Rome, Italy)
		Jan-Willem den Herder (SRON, Netherlands)
	Japanese P.I.:	Takaya Ohashi (Tokyo Metropolitan University, Japan)
EVE		
	European P.I.:	Eric Chassefière (IPSL, France)
	Japanese P.I.:	Takeshi Imamura (JAXA, Japan)
LAPLACE		
	European P.I.:	Michel Blanc (CESR, France)
	Japanese P.I.:	Sho Sasaki (National Astronomical Observatory, Japan)
MARCO POLO		
	European P.I.:	Antonella Barucci (Paris Observatory, France)
	Japanese P.I.:	Makoto Yoshikawa (JAXA, Japan)
SPICA		
	European P.I.:	Bruce Swinyard (RAL, UK)
	Japanese P.I.:	Takao Nakagawa (JAXA, Japan)
XEUS		
	European P.I.:	Martin Turner (University of Leicester, United Kingdom)
		Guenther Hasinger (MPE Garching, Germany)
	Japanese P.I.:	Hideyo Kunieda (Nagoya University, Japan)

Japan Aerospace Exploration Agency
Marunouchi Kitaguchi Building, 1-6-5, Marunouchi, Chiyoda-ku, Tokyo 100-8260 Japan
Tel:81 3 6266 6001 Fax 3 6266 6901



18 June 2007

Dr Sergio Volonté
Head
Science Planning and Community Coordination Office
European Space Agency
8-10 rue Mario Nikis
F-75738 Paris Cedex 15
France

Dear Dr Volonté,

Letter of Commitment for XEUS

This is a letter of commitment from ISAS/JAXA for the following proposal submitted to ESA in response to "Cosmic Vision 2015-2025 Call for Proposals" issued on 05 Mar 2007.

Mission Name:	XEUS
European P.I.:	Martin Turner (University of Leicester, United Kingdom) Guenther Hasinger (MPE Garching, Germany)
Japanese P.I.:	Hideyo Kunieda (Nagoya University, Japan)

ISAS/JAXA and Japanese X-ray community have been involved in the discussion and development of the XEUS mission planning in these past 8 years, by joining with ESA in the XEUS Science Advisory Group, and in the working groups, set up by that group, for telescopes, instruments and astrophysics. ISAS/JAXA has also participated in joint studies of the mission concept including the Detector Spacecraft. Since the possible areas in which we, the Japanese community, can contribute are, at system level, the Detector Spacecraft and the cryogenic chain, and for payload items, the X-ray telescopes, and detectors, we intend to support the study activity of these areas in Japan. Once the project goes into its next steps, such as phase A and B, we will make our best efforts to obtain the budget to implement developments in most of, or part of, the areas mentioned above.

ISAS/JAXA recognizes the scientific importance of XEUS, and will support the study activity by the Japanese team during the assessment phase, if the proposal is successfully selected. The commitment for the following phases is subject to the availability of funds, but ISAS/JAXA will make its best effort to promote and to support the project, if it goes into later phases successfully.

Best Regards,

A handwritten signature in black ink, appearing to read 'Hajime Inoue'.

Hajime Inoue
Executive Director
Institute of Space and Astronautical Science (ISAS)

Institute of Space Astronautical Science
Japan Aerospace Exploration Agency
3-1-1 Yoshinodai Sagamihara, Kanagawa, 229-8510 Japan Tel: 81 42-759-8000

ФЕДЕРАЛЬНОЕ КОСМИЧЕСКОЕ АГЕНТСТВО
Щепкина ул., 42, Москва, РОССИЯ, ГСП-6, 107996 Факс 688-90-63, 975-44-67 Тел. 631-94-44

FEDERAL SPACE AGENCY
42 Shepkina st., Moscow RUSSIA, GSP-6, 107996 Fax 688-90-63, 975-44-67 Phone 631-94-44

*УМ-40-4156
05.06.2007*

Директору ЕКА по научным
вопросам
Профессору Дэвиду Соусвуду.
ФАКС : 33 1 5369 7560

На дек. от 5.03.2007 № D/SCI/22639

Глубокоуважаемый профессор Соусвуд!

Настоящим письмом подтверждаем участие российских ученых в предложении «X-ray Evolving Universe Spectroscopy» (XEUS) (спектроскопия излучающей в рентгеновском диапазоне длин волн Вселенной), которое подготовлено в рамках объявленного ЕКА сбора заявок по программе Cosmic Vision 2015-2025.

Роскосмос проинформирован о предлагаемом исследовании и поддерживает возможность сделать новый значительный шаг в понимании эволюции излучающей Вселенной, черных дыр и крупномасштабной структуры Вселенной. Концепция построения телескопа XEUS при помощи отдельных спутников, или для легких зеркал и другой для фокальных детекторов является новаторской и требует серьезных технологических разработок.

В случае отбора ЕКА миссии XEUS для отечественной стадии, Роскосмос поддержит эту фазу более детальной проработкой возможного вклада России в эту миссию в виде космической платформы для рентгеновских зеркал и вклада в фокальные детекторы.

Заместитель руководителя

с уважением


Ю.И.Носенко

To: Professor David Southwood
Director of Science (D/SCI)
European Space Agency
Fax: +33 (1) 5369-7560

Reply on Ref. D/SCI/22639, 5.03.2007

Dear Professor Southwood!

Herewith we endorse the participation of Russian scientists in the «X-ray Evolving Universe Spectroscopy» (XEUS) proposal in response to the ESA Cosmic Vision 2015-2025 call for mission proposals.

Roscosmos is aware of the proposed investigation and supports the possibility to reach a major new step in the understanding of the evolution of the violent Universe, black holes and the large scale structure. The formation-flying concept of the XEUS telescope, with separate spacecrafts for the light-weight mirrors and the for the focal plane detectors is highly innovative and technologically challenging.

In case the XEUS mission is selected for an Assessment Phase by ESA, Roscosmos will support this Phase with more detailed study of possible Russian contribution in this mission, in particular a space platform for X-ray mirrors and contributions to the focal plane detectors.

Deputy Head of Roscosmos

Yu.I. Nosenko



Schweizerische Eidgenossenschaft
Confédération suisse
Confederazione Svizzera
Confederaziun svizra

Swiss Confederation

Federal Department of Home Affairs FDHA
State Secretariat for Education and Research SER
Swiss Space Office

CH-3003 Bern, SER

Dr. Sergio Volonté
ESA HQ
Science Planning and Community
Coordination Office
8-10 Marlo-Nikis
F-75738 Paris Cedex 15

Reference: 912.4501
Your Ref:
Our Ref.: FR
Official in charge: Jakob Frauchiger
Bern, 14 June 2007

**Call for Proposals of Cosmic Vision 2015-2025
Awareness of potential contributions from Switzerland in the field of scientific ground segment**

Dear Dr. Volonté,

With this letter, the Swiss Delegation confirms its awareness of Swiss scientists being involved in the development of concepts for the scientific ground segment for mission proposals in answer to the call for Proposals of Cosmic Vision 2015-2025.

For at least one of these missions (XEUS), the scientific ground segment is based on concepts that evolve from the experiences gained at the Geneva Integral Science Data Centre (ISDC) in the frame of the INTEGRAL mission. The kernel of this concept is that a set of services to the community is provided by the community and is largely funded through national agencies.

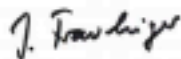
We have been informed by the scientists of the ISDC that they intend to contribute very significantly to the efforts related to the science ground segment of either of these missions to the extent that they would be ready to lead them. This involvement will lead to the submission of funding requests to the Federal Space funding authorities by ISDC for the coming years. The timescale, the total required effort and the organisation of international consortia are not known yet, as they depend on the Cosmic Vision selection process.

Based on the success of the Swiss involvement in the INTEGRAL science ground segment, and in view of the above, we want to express with this letter that we will consider very constructively a continuation of our support to activities in this field.

Should mission proposals involving the Geneva science ground segment be selected by ESA for implementation in the Cosmic Vision 2015-2025 Programme, the Swiss Space Office in a very constructive way will enter procedures with the goal to support also nationally the aforementioned contributions with Swiss entities. Funding for an initial development phase would be on the request of future PIs or Co-Is via the optional ESA Programme Prodex. All possible funding allocations will be subject to national rules and procedures and the availability of funds.

Sincerely

State Secretariat for Education and Research SER



Jakob Frauchiger
Scientific Programmes Manager

Copies to:

- Director of the ESA Science Programme: Prof. David Southwood
- Principle Investigator XEUS:
Dr Martin Turner
Space Research Centre
University of Leicester
University Road
Leicester LE1 7RH
United Kingdom
- SSO

Dr. Sergio Volonte
European Space Agency
8-10 Rue Mario Nikis
F-75738 Paris Cedex 15
France
Fax: +33 (1) 5369-7236

Dear Dr. Sergio Volonte,

In recognizing, (1) the strong scientific interests of China's space astronomy community, in particular the team led by Prof. Shuang-Nan Zhang of the Institute of High Energy Physics, Chinese Academy of Sciences and Tsinghua University, to the XEUS mission, and (2) the excellent match between this mission's main scientific objectives and China's road map for space astronomy in the next 15 years or so, China Academy of Space Technology (CAST) is interested in participating in building the platforms for both mirror and detector spacecrafts (excluding mirrors and detectors), as well the formation flying system for the XEUS mission, provided that an agreement is reached between ESA and China's National Space Administration (CNSA) and that funding for these tasks is provided by CNSA beyond the Phase-A study of this mission.

Should the XEUS mission is selected by ESA for further study, our initial study on the two platforms and formation flying system will be carried out with internal funding support from CAST. We anticipate that an initial discussion on our participation in the XEUS mission will be made during the currently planned meeting in September this year in Beijing between CNSA and ESA.

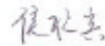
Sincerely yours,



Wangli Ph.D., Director
Deep Space Exploration@Science Technology Research Division
Research & Development Center
China Academy of Space Technology

Add: No.104, Youyi St., Haidian, Beijing, China
P.O Box: 5142-109, Beijing, China
Zip Code: 100094

Tel : (8610)68747472
Fax: (8610)68747464
Mobile: 13321197926
Email: Wangli@cast.cn



HouXinbin Ph.D.

Tel : (8610)68747308
Fax: (8610)68747464
Mobile: 13161568788
Email: Houxinbin@cast.cn

National Aeronautics and
Space Administration
Headquarters
Washington, DC 20546-0001



JUN - 8 2007

Reply to A/In of:

Science Mission Directorate

NASA has received a description of the following mission, which has been identified as a mission that will be proposed to the European Space Agency (ESA) for consideration as a Cosmic Vision mission, as well as a description of the mission's science objectives.

Mission: X-ray Evolving Universe Spectroscopy (XEUS) mission

Letter requested by: Richard E. Griffiths (Carnegie Mellon University)

NASA is aware of this proposal and acknowledges that its science objectives are aligned with the Science Plan for NASA's Science Mission Directorate 2007-2016 (also referred to as NASA's 2007 Science Plan).

This letter may be included in the proposal that is submitted to ESA. NASA has not provided ESA with a copy of this letter. NASA will enter into discussions with ESA about support of selected proposals at an appropriate time.

Sincerely,

A handwritten signature in black ink, appearing to read "S. Alan Stern".

S. Alan Stern
Associate Administrator for
Science Mission Directorate